Revisiting Siegert Pseudostates Method for Calculation of Resonances

Pankaj Kumar Jangid
(MS16140)

A dissertation submitted for the partial fulfillment of BS-MS dual degree in Science

Indian Institute of Science Education and Research Mohali
April 2021

Revisiting Siegert Pseudostates Method for Calculation of Resonances

Pankaj Kumar Jangid
(MS16140)

May 6, 2021
Version: Final submission

Indian Institute of Science Education and Research, Mohali

Department of Chemical Sciences

Master Thesis

Revisiting Siegert Pseudostates Method for Calculation of Resonances

Pankaj Kumar Jangid

(MS16140)

1. Reviewer Dr. R. Ramesh
Department of Chemical Sciences
IISER Mohali

2. Reviewer Dr. K. R. Shamasundar
Department of Chemical Sciences
IISER Mohali

Supervisor Dr. P. Balanarayan

May 6, 2021

Pankaj Kumar Jangid
Revisiting Siegert Pseudostates Method for Calculation of Resonances
Master Thesis, May 6, 2021
Reviewers: Dr. R. Ramesh and Dr. K. R. Shamasundar
Supervisor: Dr. P. Balanarayan

Indian Institute of Science Education and Research, Mohali
Department of Chemical Sciences
Knowledge city, Sector 81, SAS Nagar, Manauli
140306 and Mohali

Certificate

This is to certify that the dissertation titled "Revisiting Siegert Pseudostates Method for Calculation of Resonances" submitted by Mr. Pankaj Kumar Jangid (Reg. No. MS16140) for the partial ful- filment of BS-MS dual degree programme of the Institute,IISER Mohali, has been examined by the thesis committee duly appointed by the Institute. The committee finds the work done by the candidate satisfactory and recommends that the report be accepted.

Dr. R. Ramesh	Dr. K. R. Shamasundar	Dr. P. Balanarayan (Supervisor)

Date : May 6, 2021

Declaration

I declare that this thesis is record of work carried out by me under supervision of Dr. P. Balanarayan , Assistant Professor, IISER Mohali. I further declare that this thesis has not previously formed the basis for the award of any degree, diploma, fellowship or other similar title of recognition.

Mohali, May 6, 2021

Pankaj Kumar Jangid

In my capacity as the supervisor of the candidate's project work, I certify that the above statements by the candidate are true to the best of my knowledge.

Mohali, May 6, 2021

Dr. P. Balanarayan
(Supervisor)

Acknowledgement

I wish to express my heartiest gratitude to my thesis supervisor Dr. P. Balanarayan, Assistant professor, IISER Mohali, who gave me valuable time to guide and supervise me on this thesis.

Many deepest appreciations to Prashant Raj for his guidance and support throughout the thesis.

I am grateful to the Indian Institute of Science Education and Research(IISER) Mohali for providing such an environment of learning and Library (IISER Mohali) for providing access to various journal articles and computer facilities .

I am also thankful to all the friends and family for their kind support.

Abstract

Siegert pseudostates(SPS) are defined as the solutions of Schrödinger equation for cutoff potentials satisfying outgoing boundary condition. The problem of solving boundary value problem is then reduced to standard eigenvalue problem which can be easily solved on computers. For sufficiently large number of basis functions and cutoff radius the SPSs include bound states, antibound states, resonant states and continuum. From a radial problem, the SPS formulation is extended to a full one-dimensional axis problem. The computational efficiency of this method is then illustrated by a number of model problems. To explain the quantum mechanical tunneling of resonance states, calculated by SPS method, phase space quasiprobability distribution functions : Wigner distribution and the Husimi distribution are calculated. The negative regions appeared in the Wigner distribution represent the interference pattern and tunneling involved in the resonance and anti-resoanance states. From these distributions the grwoing and decaying nature of resonance and anti-resonance states can be explained.

Contents

1 Introduction

> *You cannot do better design with a computer, but you can speed up your work enormously.*
>
> — **Wim Crouwel**
> (Graphic designer and typographer)

Resonance phenomena are very important and have been studied extensively for a long time. Many texts introduce resonant states as poles of the scattering matrix. Despite their long history, resonance phenomena have recently become increasingly important, especially in the quantum mechanics of mesoscopic devices. Such devices can be open quantum systems and the dynamics here proceeds through resonant states. Such resonant conduction of mesoscopic systems has been extensively studied experimentally Reference[1].

Resonances can be viewed as temporarily localized wave packets. These resonances correspond to pre-dissociating, metastable states characterized by an energy E_r and a width Γ_r. The width is related to the lifetime τ by the energy-time uncertainty $\tau = \hbar/\Gamma$. In a time-dependent picture, resonances can be viewed as localized wave packets made by superposition of the continuum states, where $\tau = \hbar/\Gamma$ qualitatively resembles quasi bound states. In this chapter, we will introduce shape-type and Feshbach-type resonances.

1.1 Shape-type resonances

These type of resonances are associated with the shape of the potential in which the particle has to tunnel through a barrier[2]. In this type of resonance the shape of the potential heavily affects the rate of decay of a resonance state. A simple example of this is the potential barrier induced by a diatomic molecule's rotation motion about its center of mass. The potential energy curve of H_2 molecule within the framework of the Born-Oppenheimer approximation is given by:

$$V_J(r) = D(1 - \exp(-\alpha(r - r_0)))^2 + \frac{J(J+1)}{\mu r^2} \tag{1.1}$$

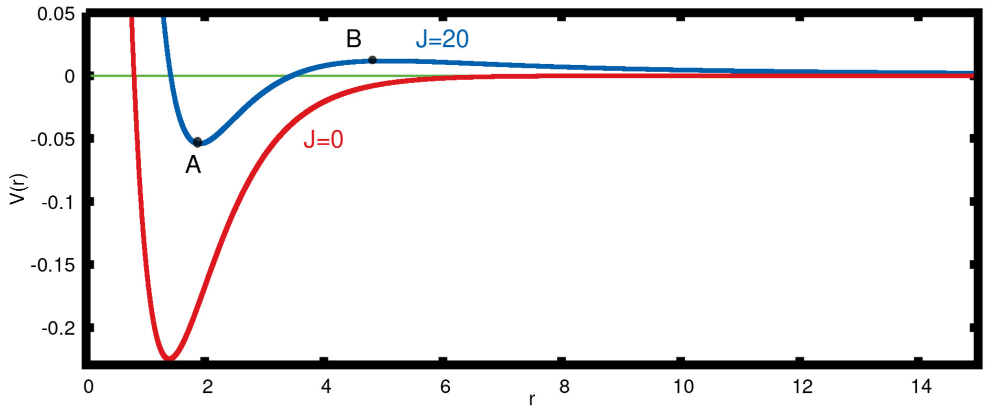

Fig. 1.1.: Ground state electronic energy of He_2, as a function of internuclear distance r and for different values of angular momentum

The form of potential is Morse type potential with an extra term representing centrifugal potential. Here r is internuclear distance, $D = 0.225$, $\alpha = 1.174$, $r_0 = 1.40$ and reduced mass $\mu = 918.735$. All quantities are given in atomic units. The rotational quantum number J has values $J = 0, 1, 2, \cdots$. The Morsh potential part represents the diatomic molecule's electronic energy in its ground state as a function of internuclear distance r.

With an increase in the rotational quantum number, a potential rotational barrier emerges. In Fig. 1.1 the point A in the potential energy curve is the local minimum, and point B is the local maximum for rotationally excited state. The classical dissociation energy is the difference between two extremum points. Rotationally excited vibrational states which are located above the threshold can tunnel through the potential barrier and dissociate. This dissociation of a molecule with lesser energy than the classical dissociation is called pre-dissociation.

1.2 Feshbach resonances

Feshbach resonances are obtained for many-particle or a single particle in an $n-$dimensional potential where $n > 1$. The Feshbach resonance states can be described as a bound states which are coupled to the continuum. This bound state then becomes metastable or quasistationary due to the coupling with the continuum. This state has a finite lifetime and, as time passes, decays to the reaction products.

To understand the physics of Feshbach resonance, we use alkali metal atoms to illustrate the main ideas. The ground state electronic structure of alkali metal atoms

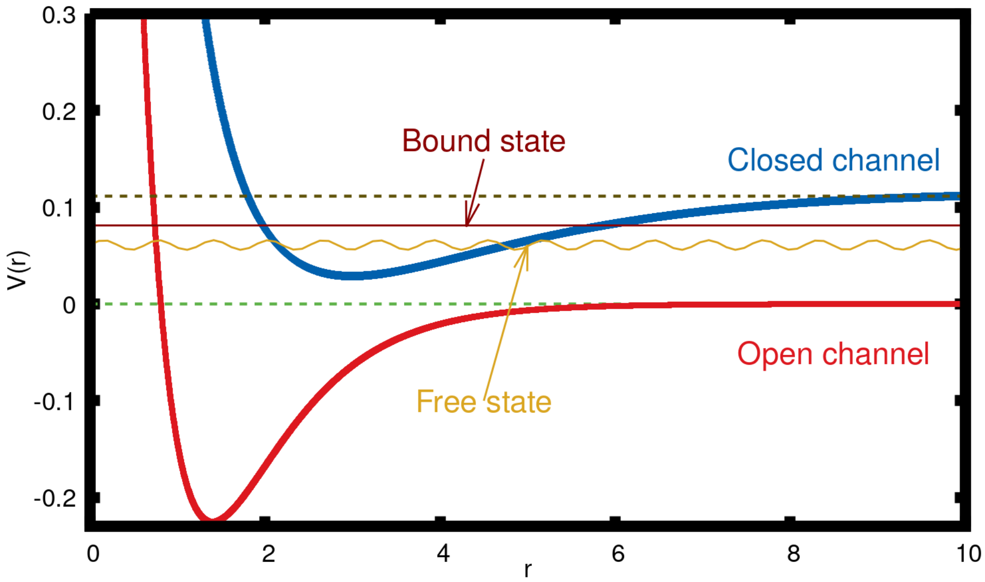

Fig. 1.2.: Illustration of the Feshbach resonance

is such that all electronic shells are filled, and there is only a single valence electron in the highest occupied shell. Alkali atoms have a nuclear spin **I** that couples to the electronic spin by hyperfine interactions. For the alkali atoms, electrons have zero orbital angular momentum, and the coupling arises only because of the electronic spin **S**. So the value of total spin is $\mathbf{F} = \mathbf{I} + \mathbf{S}$. With an applied magnetic field, the levels are split because of the hyperfine interactions. With an external magnetic field applied, the energy levels are further split because of the interactions of electron's magnetic moments and the nucleus with a magnetic field.

In Fig.1.2 there are two types of interaction potential named as "open channel" and "closed channel". When atoms are far apart, and their spin configuration is such that they see the interaction potential of the open channel. Due to the exchange coupling, the spin of one of the colliding atoms gets flipped, so in this different spin arrangement, atoms see a different interaction potential named as a closed channel. Generally, the closed channel potential has bound states and let's assume that there is one bound state with energy E_m which is close to the open channel continuum. When a magnetic field is applied at a certain value of the magnetic field, the coupling of this bound state of the closed channel continuum of the open channel is maximum. The applied magnetic field at resonance defines the resonance position.

By this Feshbach resonance mechanism, the atom-atom interactions can be made attractive or repulsive, very large or very small, thus modifying the properties of the gas.

1.3 Siegert states

While deriving the Breit Wigner formula for nuclear reactions, Siegert explained some singularity conditions in the scattering cross-section[3]. Those singularities which lie near enough to the real axis cause a sharp resonance maximum in the cross-section. Since singularity in scattering cross-section also implies a singularity in the scattering matrix and a sharp peak appears at the resonance position. Siegert states satisfy outgoing boundary conditions for the s-wave scattering problem.

Consider Schrödinger equation given by

$$(\hat{H} - E)\phi(r) = 0, \qquad \hat{H} = -\frac{1}{2}\frac{d^2}{dr^2} + \hat{V}(r) \tag{1.2}$$

Here potential is short ranged which vanishes as $r \to \infty$. Siegert states are defined as the solutions to Eq. (1.2) which satisfy the boundary conditions given by

$$\phi(0) = 0 \qquad \text{at} \qquad r = 0 \tag{1.3}$$

and the outgoing boundary condition at $r \to \infty$,

$$\left(\frac{d}{dr} - ik\right)\phi(r)\bigg|_{r\to\infty} = 0 \tag{1.4}$$

Here momentum, k, and energy are related by

$$E = \frac{1}{2}k^2 \tag{1.5}$$

In Schrödinger equation, Eq. (1.2), momentum appears quadratically, and in the boundary condition, Eq. (1.4), it appears linearly, so these equations can be solved only iteratively with some initial guess. By the iterative process, only one state can be solved at a time.
Here are some properties associated with momentum values calculated from Siegert states.

- Siegert states can be satisfied simultaneously only for a discrete set of generally complex mementum k_n.

- The values k_n coincide with the poles of the scattering matrix in the complex k plane.
- The values of k_n for which Re(k_n)=0 correspond to bound and antibound states.
- Momentum with $Re(k_n) \neq 0$ can only appear in the lower half of the complex k plane.

The solution of Siegert states can be evaluated by considering the problem as a differential equation and solving it iteratively for each state. In order to achieve the completeness required for representing the continuum, one has to generate not just one or a few but many solutions of Siegert states. This causes an essential practical difficulty in handling the Siegert states.
The Siegert pseudostate formulation proposed by Tolstikhin, Ortrovsky and Nakamura [4,5] eliminates the problem of evaluation of Siegert states by the modified boundary conditions. In this method, the boundary condition is applied at a finite distance that makes the application of finite basis feasible. Utilizing finite basis expansion, the problem is reduced to an eigenvalue problem. In this method, computational labor is reduced essentially to that of a single matrix diagonalization.

Bibliography

[1] S. Datta, Electronic Transport in Mesoscopic Systems(Cambridge University Press, Cambridge, 1995)

[2] Nimrod Moiseyev, *Non-Hermitian Quantum Mechanics* (Cambridge University Press, 2011)

[3] A. J. F. Siegert, Phys. Rev. **56**, 750 (1939).

[4] O. I. Tolstikhin, V. N. Ostrovsky, and H. Nakamura, Phys. Rev. Lett. **79**, 2026 (1997).

[5] O. I. Tolstikhin, V. N. Ostrovsky, and H. Nakamura, Phys. Rev. A **58**, 2077 (1998).

[6] Josep Taron, American Journal of Physics **81**, 603 (2013)

[7] Progress of Theoretical Physics, Vol. 119, No. 2, February 2008

2 Siegert Pseudostate Formulation

> *A picture is worth a thousand words. An interface is worth a thousand pictures.*
>
> — **Ben Shneiderman**
> (Professor for Computer Science)

The inefficiency of computation of Siegert states[1] provides a great scope to work with the new mathematical idea of Tolstikhin *et al.*[2][3] In the Siegert pseudostate method the outgoing boundary condition is applied only to a finite point

$$\left(\frac{d}{dr} - ik\right)\phi(r)\bigg|_{r\to a} = 0 \tag{2.1}$$

with some simplifications used to convert the Schrödinger equation to an eigenvalue problem. In this case the potential $V(r)$ is taken for a finite value $r = a$ and for $r > a$ it is assumed to be zero. The solutions to these equations are termed Siegert pseudostates(SPS)[2]. This cutting off the potential can lead to two possibilities -

First, if the potential $V(r)$ vanishes for a finite value of r, then SPS coincides with Siegert states for a sufficiently large a. Second, if the value of potential $V(r)$ does not vanish for large r, then SPS also depends upon the cutoff radius, and these are quite different from the exact Siegert states.

In this chapter we discuss the mathematical aspects of Siegert pseudostate method and learn how this method is computation friendly.

2.1 Boundary value problem in algebraic form

Reduction of cutoff boundary is very important to implement the method practically. We expand the solutions of the SSCPs in terms of some square-integrable basis, which reduces the differential equation to an algebraic form. For this a finite basis employed is given by:

$$\pi_i(r), \qquad i = 1, 2, 3, \cdots, N \tag{2.2}$$

which is assumed to be orthonormal on the interval $[0, a]$,

$$\int_0^a \pi_i(r)\pi_j(r)dr = 0, \tag{2.3}$$

and becomes complete when $N \to \infty$

$$\sum_{i=0}^{N} \pi_i(r)\pi_i(r') = \mathbf{I} \tag{2.4}$$

It is assumed that $\pi_i(0) = 0$, but no restriction is imposed near $r = a$. From the Eq. (1.2), (1.3), and (1.5)

$$\left(-\frac{1}{2}\frac{d^2}{dr^2} + \hat{V}(r) - E\right)\phi(r) = 0 \tag{2.5}$$

Premultiplying this equation by $\pi_i(r)$ and integrating over $r \in [0, a]$

$$-\frac{1}{2}\int_0^a \pi_i(r)\frac{d^2\phi(r)}{dr^2}dr + \int_0^a \pi_i(r)\hat{V}(r)\phi(r)dr - E\int_0^a \pi_i(r)\phi(r)dr = 0 \tag{2.6}$$

Solving first term by part and applying boundary conditions given by Eq.(2.1)

$$\begin{aligned}\left[-\frac{1}{2}\pi_i(r)\frac{d\phi(r)}{dr}\right]_0^a + \frac{1}{2}\int_0^a \frac{d\pi_i(r)}{dr}\frac{d\phi(r)}{dr}dr + \int_0^a \pi_i(r)\hat{V}(r)\phi(r)dr \\ - E\int_0^a \pi_i(r)\phi(r)dr = 0\end{aligned} \tag{2.7}$$

$$\Rightarrow \frac{1}{2}\int_0^a \frac{d\pi_i(r)}{dr}\frac{d\phi(r)}{dr}dr - \frac{ik}{2}\pi_i(r)\phi(r) + \int_0^a \pi_i(r)(\hat{V}(r) - E)\phi(r)dr = 0 \tag{2.8}$$

Only the values of $\phi(r)$ for r within the interval $[0, a]$ appear in this equation. Hence we can expand $\phi(r)$ in Eq.(2.8) in terms of the basis

$$\phi(r) = \sum_{j=0}^{N} c_j\pi_j(r), \qquad 0 \le r \le a. \tag{2.9}$$

Substituting this expansion in Eq.(2.8) we arrive at the algebraic equation

$$\left(\tilde{\mathbf{H}} - \frac{ik}{2}\mathbf{L} - \frac{k^2}{2}\mathbf{I}\right)\mathbf{c} = 0 \tag{2.10}$$

Here uppercase boldface characters represent matrices. $\mathbf{c}$ is matrix formed from coefficient vectors in Eq. (2.9). $\mathbf{I}$ is identity matrix and elements of $\tilde{\mathbf{H}}$ and $\mathbf{L}$ are given by

$$\tilde{H}_{i,j} = \frac{1}{2}\int_0^a \frac{d\pi_i(r)}{dr}\frac{d\phi(r)}{dr}dr + \int_0^a \pi_i(r)\hat{V}(r)\phi(r)dr \tag{2.11}$$

and

$$L_{ij} = \pi_i(a)\pi_j(a) \tag{2.12}$$

Now we introduce Bloch operator given by

$$\hat{L} = \frac{1}{2}\delta(r-a)\frac{d}{dr} \tag{2.13}$$

The Bloch-operator is derived by expanding the wave functions and their derivatives in terms of a complete set of orthonormal continuous functions and their derivatives defined within an internal region. Then we can write the Hermitized Hamiltonian

$$\tilde{H} = -\frac{1}{2}\frac{d^2}{dr^2} + \hat{V}(r) + \hat{L} \tag{2.14}$$

From this equation we can say that $\tilde{H}$ is a matrix representation of $\hat{H}$ within the basis. The action of L on SPS is defined by

$$\int_0^a \pi_i(r)\hat{L}\phi(r)dr = \frac{ik}{2}\pi_i(a)\phi(a) \tag{2.15}$$

By the construction itself we can see that the matrices $\tilde{\mathbf{H}}$ and $\mathbf{L}$ are real and symmetric.

2.2 Linearization of algebraic equation

Eq. (2.10) is a nonlinear eigenvalue problem. This equation can have non trivial solutions only for a discrete set of $k = k_n$; thus this can be taken as an eigenvalue problem defining k_n and corresponding eigenvectors $\vec{c}_n$. This unconventional eigenvalue problem cannot be solved by standard methods of linear algebra. To solve such type of equations we consider a quadratic eigenvalue problem

$$\left(\mathbf{A} + \lambda\mathbf{B} + \lambda^2\mathbf{I}\right)\mathbf{c} = 0 \tag{2.16}$$

where $\mathbf{I}$ is an identity matrix and $\mathbf{A}$ and $\mathbf{B}$ are some square matrices of dimension $N \times N$, solution of the eigenvalue problem gives eigenvalues λ, and eigenvectors $\mathbf{c}$. This equation is related to Eq. (2.10) by the equations

$$\mathbf{A} = 2\tilde{\mathbf{H}}, \qquad \mathbf{B} = -\mathbf{L}, \qquad \lambda = ik \tag{2.17}$$

Consider a matrix polynomial of the form

$$\mathbf{M}(\lambda) = \mathbf{A} + \lambda\mathbf{B} + \lambda^2\mathbf{I} \tag{2.18}$$

From conventional methods of solving eigenvalue problem det[$\mathbf{M}(\lambda)$]= 0, is the solution of all eigenvalues. We observe that quadratic matrix polynomial has exactly $2N$ eigenvalues. Thus, for a given N there are $2N$ Siegert pseudostates. Considering a new equation which is always true

$$\mathbf{0c} + \mathbf{I}\tilde{\mathbf{c}} = \lambda\mathbf{Ic} \tag{2.19}$$

and are write Eq.(2.18) in a different form

$$-\mathbf{Ac} - \mathbf{B}\tilde{\mathbf{c}} = \lambda\mathbf{I}\tilde{\mathbf{c}} \tag{2.20}$$

Here $\tilde{\mathbf{c}} = \lambda\mathbf{c}$. Then Eq. (2.19) and Eq. (2.20) form a system of equations which are a discrete analog of reducing a second order differential equation to a set of first order equations. Hence can be written in the form of a matrix

$$\begin{pmatrix} \mathbf{0} & \mathbf{I} \\ -\mathbf{A} & -\mathbf{B} \end{pmatrix} \begin{pmatrix} \mathbf{c} \\ \tilde{\mathbf{c}} \end{pmatrix} = \lambda \begin{pmatrix} \mathbf{c} \\ \tilde{\mathbf{c}} \end{pmatrix} \tag{2.21}$$

This is also an eigenvalue problem, but in comparison to Eq. (2.16), this is a linear problem and can be dealt easily. The size of matrix in Eq. (2.21) is $2N \times 2N$ hence given $2N$ eigenvalues λ_n, which conside with $2N$ eigenvectors. Despite being linear eigenvalue problem, matrix form in Eq.(2.21) is not symmetric and can be symmetrized by pre-multiplying with the matrix

$$\begin{pmatrix} \mathbf{B} & \mathbf{I} \\ \mathbf{I} & \mathbf{0} \end{pmatrix} \tag{2.22}$$

The resultant equation is

$$\begin{pmatrix} -\mathbf{A} & \mathbf{0} \\ \mathbf{0} & \mathbf{I} \end{pmatrix} \begin{pmatrix} \mathbf{c} \\ \tilde{\mathbf{c}} \end{pmatrix} = \lambda \begin{pmatrix} \mathbf{B} & \mathbf{I} \\ \mathbf{I} & \mathbf{0} \end{pmatrix} \begin{pmatrix} \mathbf{c} \\ \tilde{\mathbf{c}} \end{pmatrix} \tag{2.23}$$

If matrices **A** and **B** are symmetric, this is a generalized symmetric algebraic eigenvalue problem, and can be solved numerically.

2.3 General Properties of Eigenvalues

Since matrix **A** and **B** are real and symmetrix, we can deduce some properties of the eigenvalues k_n from matrix algebra knowledge.

- Since the nature of eigenvalue problem is quadratic its eigenvlaues λ_n can be real and complex.
- Multiplying $(\mathbf{A} + \lambda\mathbf{B} + \lambda^2\mathbf{I})\,\mathbf{c} = 0$, by $c^\dagger$ and taking the imaginary part of the result we get
$$Im(\lambda)\left[2Re(\lambda)\mathbf{c}^\dagger\mathbf{c} + \mathbf{c}^\dagger\mathbf{B}\mathbf{c}\right] = 0 \tag{2.24}$$
Eq. (2.24) is true for all solutions of the eigenvalue problem. From this equation, we can consider two types of solutions-
- First, $\mathrm{Im}(\lambda) = 0$ which means that real part of k is zero. So the values of k can be purely imaginary.
- Second, the real part of λ should be positive or the imaginary part of k should be only a negative value. This observation leads to the conclusion that eigenvalues with nonzero real part of k can only occur in the lower half of the complex k plane.

These properties coincide with the well-known properties of Siegert eigenvalues.

Bibliography

[1] A. J. F. Siegert, Phys. Rev. **56**, 750 (1939).

[2] O. I. Tolstikhin, V. N. Ostrovsky, and H. Nakamura, Phys. Rev. Lett. **79**, 2026 (1997).

[3] O. I. Tolstikhin, V. N. Ostrovsky, and H. Nakamura, Phys. Rev. A **58**, 2077 (1998).

3 Numerical Implementation of Siegert Pseudostates

> *Innovation distinguishes between a leader and a follower.*
>
> — **Steve Jobs**
> (CEO Apple Inc.)

In this chapter we describe the numerical procedure used for calculating Siegert pseudostates to treat radial type of potential as well as the potentials which span full one dimensional axis. To numerically solve the problem, we need to calculate matrix elements in Eq. (2.11) and (2.12) numerically. To calculate these matrix elements and integrals we are going to utilize the finite basis representation and discrete variable representation[1] methods.

3.1 Finite Basis Representation(FBR)

In FBR method a set of basis functions which is analytically known is considered

$$\{\varphi(x)\}_{j=1}^{n} \tag{3.1}$$

which is orthonormal $\langle\varphi_j|\varphi_k\rangle = \delta_{ij}$, and becomes complete for $n \to \infty$

$$\sum_{j=1}^{\infty} |\varphi_j\rangle\langle\varphi_k| = 1 \tag{3.2}$$

In this method matrix elements of desired operator are calculated analytically for a finite number of basis functions. We then approximate the wavefunction as

$$\psi(x) = \sum_{j=1}^{n} a_j \varphi_j(x), \qquad a_j = \langle\varphi_j|\psi\rangle \tag{3.3}$$

In the FBR method, the computation of the matrix elements of the potential

$$V_{ij} = \langle \varphi_j | V | \varphi_k \rangle = \int \varphi_j^*(x) V(x) \varphi_k(x) dx \tag{3.4}$$

requires $N(N+1)/2$ integral evaluation which is very difficult and time consuming for large basis and to do calculations for different potential we need to these integral calculations again. The discrete variable representation (DVR)[1] offers a solution to the integral problem.

3.2 Discrete Variable Representation(DVR)

DVR method makes use of both, a global basis set

$$\{\varphi(x)\}_{j=1}^{n} \tag{3.5}$$

and a set of grid points

$$\{x_\alpha\}_{\alpha=1}^{n} \tag{3.6}$$

For the current problem we employ the set of functions in $L^2[-1,1]$

$$\varphi_n(x) = \frac{1}{\sqrt{h_{n-1}}} P_{n-1}(x), \qquad n = 1, 2, \cdots, N \tag{3.7}$$

Where $P_n(x)$ are the Legendre polynomials orthogonal on the interval $x \in [-1,1]$ and h_n are corresponding normalization constants given by[2]

$$h_n = \frac{2}{2n+1} \tag{3.8}$$

Then the basis $\varphi(x)$ is orthonormal and becomes complete in $L^2[-1,1]$ when $N \to \infty$. However, in practical calculations, one can deal with only a finite number N of the basis functions. Such truncation of the basis is known as FBR, as previously discussed.

To evaluate integral of potential it is convenient to switch from the FBR to DVR method. This integral problem brings us to *Gaussian Quadrature*. General quadrature rule is formulated as

$$\int \omega(x) f(x) dx = \sum_{i=1}^{n} w_i f(x_i) \tag{3.9}$$

where $\omega(x)$ is weight function and $f(x)$ is an arbitary function such that the integral on the left-hand side of Eq. (3.9) exists and x_i and ω_i are quadrature abscissas and weights, respectively. The formula(3.9) gives exact result for $f(x)$, a polynomial of degree less than $2N$.

In our calculation some integral are exactly solvable and FBR matrix can be constructed and for some integral DVR is convenient. The quadrature and Christoffel-Darboux[3] identity provides a foundatin for the FBR-DVR transformation.

$$\pi_i(x) = \sum_{i=1}^{N} T_{ni}\varphi_n(x) \tag{3.10}$$

where

$$T_{ni} = \kappa_i \varphi_n x_i, \qquad \kappa_i = \sqrt{\frac{\omega_i}{w(x_i)}} \tag{3.11}$$

and

$$\mathbf{T}^T\mathbf{T} = \mathbf{I} \tag{3.12}$$

then we can write

$$\varphi_n(x) = \sum_{i=1}^{N} T_{ni}\pi_i(x) \tag{3.13}$$

The DVR basis functions

$$\pi_i(x), \qquad n = 1, 2, \cdots, N \tag{3.14}$$

also form and orthonormal set on the interval [-1,1]

3.3 Potential of Radial Type

To solve potential of radial type it is more convenient to consider somewhat modified form of Eqs.(1.2), (1.3), (1.5) and (1.6). In this modified form wavefunction is considered to be multiplied with r, which automatically satisfies Eq.(1.3). Then modified Schrödinger equation is given by

$$\left[\hat{H} - \frac{1}{2}k^2r^2\right]\varphi(r) = 0 \tag{3.15}$$

Here Hamiltonian H is defined by

$$\hat{H} = \hat{K} + \hat{U}(r) \tag{3.16}$$

$$\hat{K} = -\frac{1}{2}\frac{d}{dr}r^2\frac{d}{dr}, \qquad \hat{U}(r) = \frac{1}{2}l(l+1) + r^2\hat{V}(r) \tag{3.17}$$

Here l is the angular momentum. The advantage of this type of equations is that the boundary condition at $r = 0$, which is, $\phi(0) = 0$ is already satisfied. Then the final set of equations, along with boundary conditions, is

$$\left[\hat{H} - \frac{1}{2}k^2r^2\right]\phi(r) = 0 \tag{3.18}$$

$$\left(\frac{1}{r}\frac{d}{dr} - ik\right)\phi(r)\bigg|_{r=a} = 0 \tag{3.19}$$

These equations must be solved numerically after expanding the Siegert pseudostates in appropriate orthonormal basis.

3.4 Basis expansion in DVR and Matrix elements evaluation

Since the interval of our interest is [0,a], for the numerical treatment, instead of r we introduce a new variable x,

$$r = \frac{a}{2}(1+x) \tag{3.20}$$

Then the interval $r \in [0,a]$ maps onto $x \in [-1,1]$, and the basis defined by Legendre polynomial can be utilized. We can expand the solutions of Eq.(3.18), (3.19) and (3.20) in terms of the DVR basis

$$\phi(x) = \sum_{j=1}^{N} c_j\pi_j(x), \qquad -1 \le x \le 1 \tag{3.21}$$

Substituting this into Eq.(3.18), pre-multiplying by $\pi_i(x)$ and integrating over $x \in [-1,1]$, and using the boundary condition, Eq.(3.20), we arrive at the algebraic eigenvalue problem

$$\left[\tilde{\mathbf{H}} - (ika-1)\mathbf{L} - \frac{1}{2}k^2\boldsymbol{\rho}\right]\mathbf{c} = 0 \tag{3.22}$$

where c is the vector of coefficients and the boldface characters denote matrices defined with respect to the DVR basis:

$$\tilde{H}_{ij} = \tilde{K}_{ij} + U(r_i)\delta_{ij} \tag{3.23}$$

$$\tilde{K}_{ij} = \frac{1}{2}\int_{-1}^{1} \frac{d\pi_i(x)}{dx}(1+x^2)\frac{d\pi_j(x)}{dx}dx \tag{3.24}$$

$$L_{ij} = \pi_i(1)\pi_j(1), \tag{3.25}$$

$$\rho_{ij} = \frac{a^2}{2}\int_{-1}^{1} \pi_i(x)(1+x^2)\pi_j(x)dx \tag{3.26}$$

All these matrices are real and symmetric.The tilde over $\tilde{\mathbf{H}}$ and $\tilde{\mathbf{K}}$ indicates that they represent Hermitized version of the operators H and K, respectively. Matrix elements of $U(r)$, in Eq.(3.17), are calculated using quadrature. Matrix elements of $\tilde{\mathbf{K}}$ were calculated exactly in FBR basis and then transformed to DVR basis. FBR integral process is given in Appendix (A.1), here we directly give formulas. For $\tilde{\mathbf{K}}$ we have

$$\tilde{\mathbf{K}} = \mathbf{T}^T\tilde{\mathbf{K}}^{FBR}\mathbf{T} \tag{3.27}$$

where

$$\tilde{K}_{nm}^{FBR} = \varphi_n(1)\varphi_m(1)\left[2\sum_{k=1}^{n-1}\varphi_k^2(1) + \varphi_n^2(1) - \frac{1}{2}\right] \tag{3.28}$$

for $n < m$, and

$$\tilde{K}_{nn}^{FBR} = 2\varphi_n^2(1)\sum_{k=1}^{n-1}\varphi_k^2(1) + \frac{1}{2}\left(\varphi_n^2(1) - \frac{1}{2}\right) \tag{3.29}$$

and $\tilde{K}_{mn}^{FBR} = \tilde{K}_{nm}^{FBR}$.

The matrix $\boldsymbol{\rho}$ is given by

$$\rho_{ij} = \frac{a^2}{2}\left[(1+x_i)^2\delta_{ij} + \Delta(N)T_{Ni}T_{Nj}\right] \tag{3.30}$$

where

$$\Delta(N) = \frac{N^2}{4N^2-1} \tag{3.31}$$

Now we have our differential equations in algebraic form(3.23). To transform Eq.(3.23) in similar form of Eq.(2.16) we multiply Eq.(3.26) from left by $\boldsymbol{\rho}^{-1/2}$, we get

$$\left[\boldsymbol{\rho}^{-1/2}\tilde{\mathbf{H}} - (ika-1)\boldsymbol{\rho}^{-1/2}\mathbf{L} - \frac{1}{2}k^2\boldsymbol{\rho}^{1/2}\right]\mathbf{c} = 0 \tag{3.32}$$

Now we introduce a new vector of coefficients of

$$\mathbf{s} = \boldsymbol{\rho}^{1/2}\mathbf{c} \tag{3.33}$$

then

$$\mathbf{c} = \boldsymbol{\rho}^{-1/2}\mathbf{s} \tag{3.34}$$

from Eq.(3.33) and (3.35) we write

$$\left[\boldsymbol{\rho}^{-1/2}(\tilde{\mathbf{H}} + \mathbf{L})\boldsymbol{\rho}^{-1/2} - ika\boldsymbol{\rho}^{-1/2}\mathbf{L}\boldsymbol{\rho}^{-1/2} - \frac{1}{2}k^2\right]\mathbf{s} = 0 \tag{3.35}$$

and

$$\mathbf{A} = 2\boldsymbol{\rho}^{-1/2}(\tilde{\mathbf{H}} + \mathbf{L})\boldsymbol{\rho}^{-1/2} \tag{3.36}$$

$$\mathbf{B} = -2a\boldsymbol{\rho}^{-1/2}\mathbf{L}\boldsymbol{\rho}^{-1/2} \tag{3.37}$$

Here **A** and **B** are symmetric matrices. After evaluating these matrices, generalized eigenvalue can be solved for k_n and **c**.

3.5 Some model potentials

For a given potential $V(r)$ and the cutoff radius a, each SPS eigenvalue k_n converges when N grows and the lower k_n converge faster. Those k_n that are not affected by a further increment in N within a specified accuracy are basis-independent or N-converged eigenvalues, all other depend upon basis.

3.5.1 Square well potential

$$V(r) = \begin{cases} V_0, & r \leq a \\ 0, & r > a, \end{cases} \tag{3.38}$$

Here the values of parameters used are $a = 1$ and $V_0 = -112.5$, same as used in [4]. Figure 3.1(a) and 3.1(b) present the distribution of some low lying SPS eigenvalues.

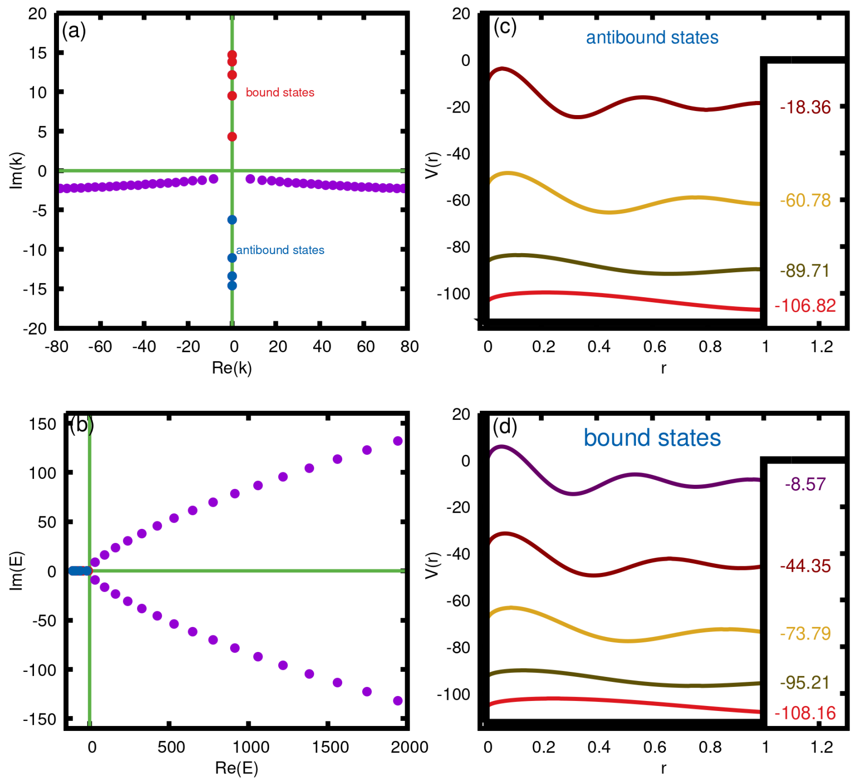

Fig. 3.1.: SPS eigenvalues and wavefunction plots for potential(3.42) with parameters $V_0 = -112.5$ and $a = 1$ calculated using $N = 200$ basis functions. (a) Complex $k-$plane. (b) Complex energy plane. (c)Potential with wavefuctions of antibound states. (d) Potential wiht wavefunctions of bound states

in complex k and E plane respectively. Figure 3.1(c) and 3.1(d) show the potential function together with wavefunctions at the energy positions for antibound and bound states, respectively. For this potential, we have tabulated 5 bound, 4 antibound states. Our calculations reproduce value with six-digit accuracy with the values listed in [4].

Tab. 3.1.: Siegert pseudostate eigenvalues for potential (3.39)

	SPS Method	Reference[4]
Bound states	14.708250193081 13.799326980103 12.148872299511 9.418482113583 4.141591892980	14.7082 13.7993 12.1489 9.41848 4.14159
Antibound states	-14.616982093458 -13.395455200471 -11.026114858494 -6.060279871637	-14.6170 -13.3955 -11.0261 -6.06028

Fig. 3.2(a) shows a larger portion of the SPS eigenvalues in the k plane, and Fig. 3.2(b) depicts the complete set. As can be seen, low-lying eigenvalues approach asymptotic results; however, after a maximum number, the dependent SPSs start diverging, forming a quite different pattern.

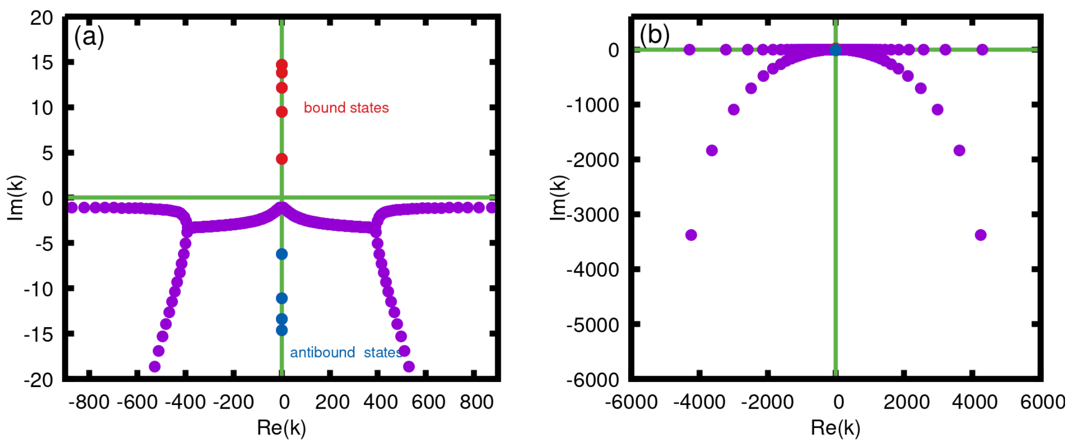

Fig. 3.2.: SPS eigenvalues for potential(3.42) with parameters $V_0 = -112.5$ and $a = 1$ calculated using $N = 200$ basis functions. (a) Larger scale (b) All eigenval

3.5.2 Smooth barrier with exponential decay

Rectangular potential calculations considered in the previous case showed high accuracy with the data given in the literature. Since the realistic potentials of interest in the collision theory usually have infinite range. In this case, we discuss a potential that has exponential decay with respect to inter-nuclear distance. We consider the potential

$$V(r) = 7.5r^2e^{-r}, \qquad 0 \leq r \leq \infty \tag{3.39}$$

which has a barrier with maximum height of ≈ 4.06 at $r = 2$. This potential produces a resonance at ≈ 3.42. Fig. 3.3(a) and 3.3(b) show distributions of some

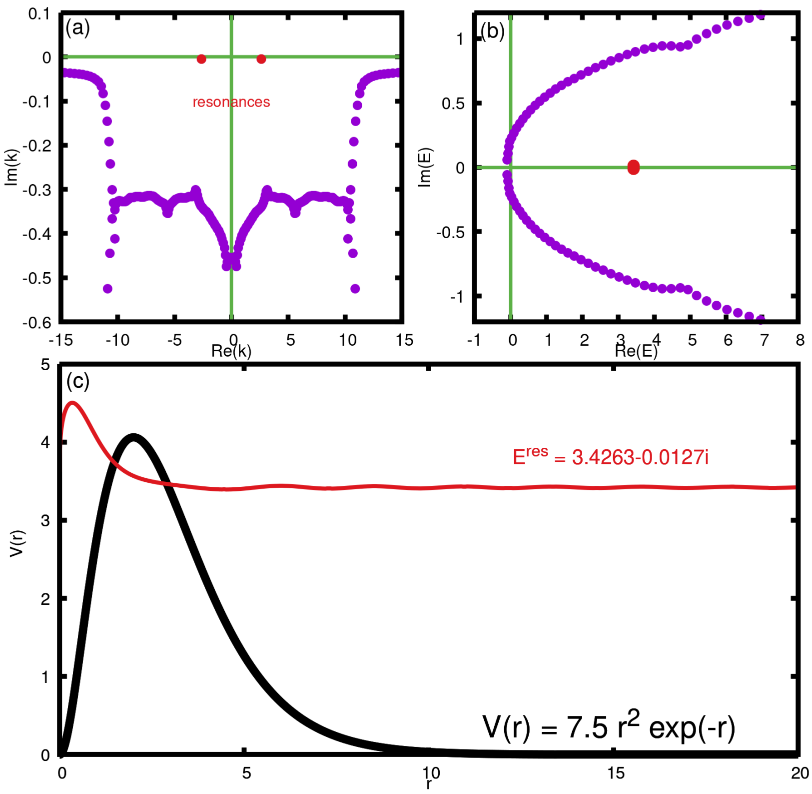

Fig. 3.3.: SPS eigenvalues and wavefunction plots for potential(3.42) with parameters $V_0 = -112.5$ and $a = 1$ calculated using $N = 200$ basis functions. (a) Complex k plane (b)Complex energy plane (c)Potential with wavefuctions of resonance states

low lying Siegert pseudostates calculated for cutoff radius a = 35 using N = 200 basis functions. Fig. 3.3(c) shows the potential function together with one resonant state wavefunction. For infinite range potentials, some of the SPS converge within specific accuracy with an increment of basis size N and cutoff radius a, and some

SPS never converge. The converging SPS corresponds to bound states, antibound states, and resonances lying close to Re(k) axis.

Resonance energy and corresponding momentum values calculated from the SPS method are listed in Tab.(3.2), along with the values calculated from the complex scaling method[6]. Eigenvalues from the SPS method are comparable with value form complex scaling.

Tab. 3.2.: Siegert pseudostate eigenvalues for potential (3.40)

	SPS Method	Complex scaling[5]
k	2.617786170321-0.004879879318i	-
E_{res}	3.426390310151-0.012774480593i	3.4262- 0.0125i

For decay type potential SPSs are more accurate for large cutoff radius. Fig. 3.4(a) depicts complex k eigenvalues for different cutoff radius showed in different colors. With the increment of cutoff radius resonant states and some low lying eigenvalues converge up to certain accuracy, and the continuum states, before divergence, start coming closer. The behavior of eigenvalue after divergence is not clear for now.

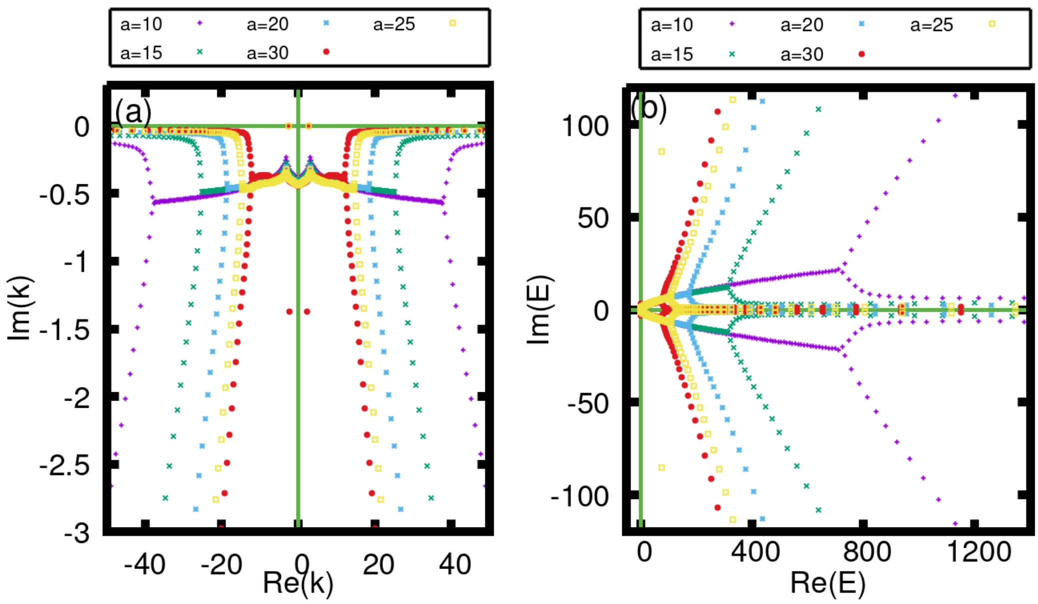

Fig. 3.4.: Complex eigenvalues for potential (3.40) for different cutoff radius a. (a) Complex k values. (b) Complex energy values.

3.5.3 Smooth barrier with Gaussian decay

In this model problem we discuss a potential which is Gaussian decay type. We consider the potential

$$V(r) = (0.5r^2 - 0.8)e^{-0.1r}, \qquad 0 \le r \le \infty \tag{3.40}$$

which has a barrier with maximum height at $r \approx 3.40$. This potential produces mainly three resonance states in which the state lying close to Re(k) axis converges very fast then the others with increment of basis size N and cutoff radius a. Figure

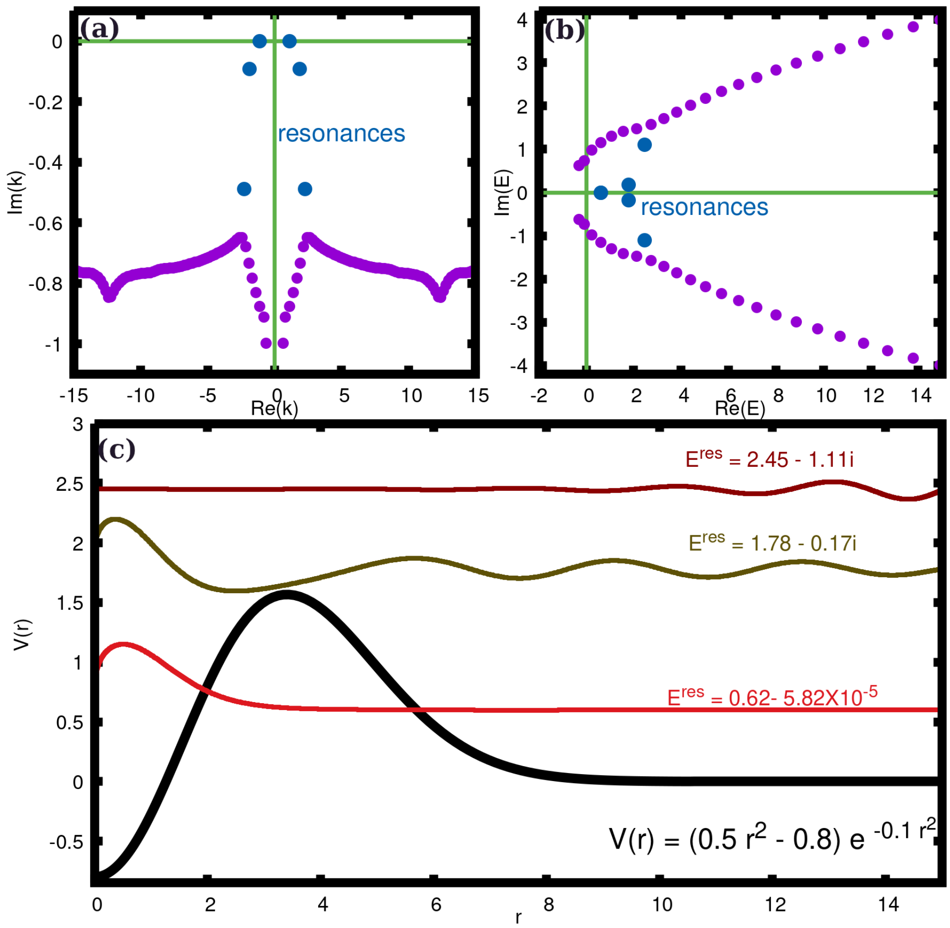

Fig. 3.5.: SPS eigenvalues and wavefunction plots for potential(3.41) with cutoff radius a = 25 calculated using N = 200 basis functions. (a) Complex-k plane. (b) Complex energy plane. (c)Potential with wavefuctions of resonance states.

3.5(a) and 3.5(b) present the distribution of some low-lying SPS eigenvalues in complex k and E plane, respectively. From these distribution, resonant states can be easily differentiated as the magnitude of their complex part is less than continuum , and in energy distribution Fig 3.5(b), they are positioned between decaying(fourth quadrant) and growing(first quadrant) branch of the continuum. Figure 3.1(c) show the potential function together with wavefunctions of resonant states.

For potential(3.41) we have tabulated the resonance states from SPS method and the energies given in Ref[5]. We have seen the behavior of eigenvalues for different

Tab. 3.3.: Siegert pseudostate eigenvalues for potential (3.41)

	SPS Method	Ref[6]
E_{res}	0.620970939655 - 0.000058266636i 1.784582848890 - 0.173750719112i 2.451641547601 - 1.102731605100i	- 1.784582 - 0.173750i 2.455696 - 1.111399i

cutoff radius a; now, we explore the effect of basis size on eigenvalue distribution. Fig. 3.6(a) depicts complex k eigenvalues for a different number of basis functions. For large and large basis , resonant states get converged up to certain accuracy, but continuum also converges. In the energy plot, Fig. 3.6(b), we can see that with an increment of basis, the converging branch of continuum starts extending in real energy axis which means more and more eigenvalues, which are supposed to converge for very large basis size, are being added to SPSs.

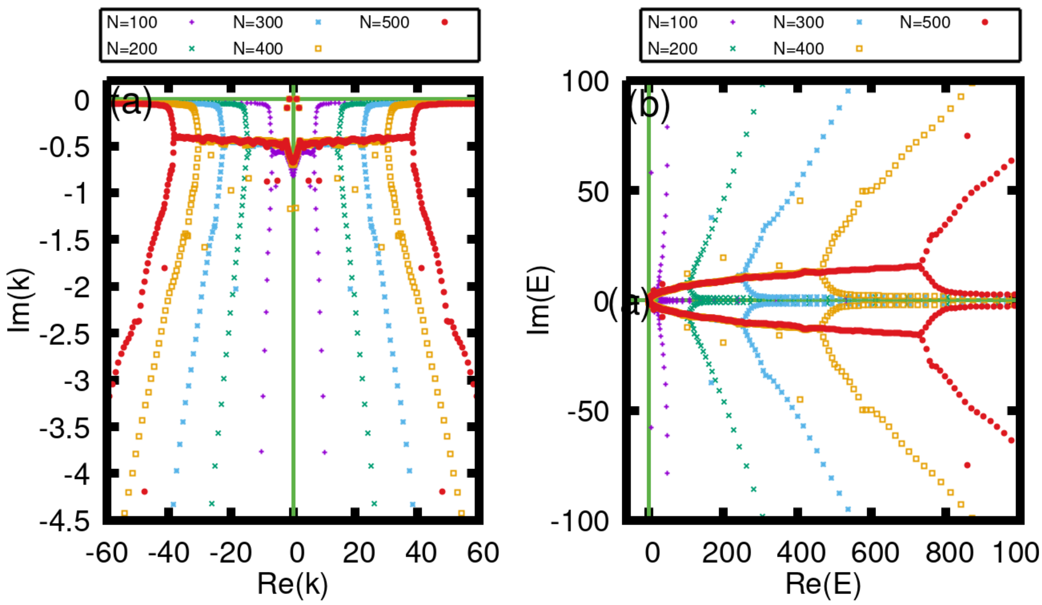

Fig. 3.6.: Complex eigenvalues plane for different values of basis functions N . (a)Complex k plane. (b) Complex energy plane

3.6 Full axis type potentials

In the radial problem considered previously, the spatial variable is restricted to a half of the axis, with the zero boundary condition at the origin. In this section, the formulation will be extended to the whole axis problem. Although the extension is almost straightforward, the formulations are not identical. Here the possibility for the waves to be ejected in two different directions in one axis is considered. The whole axis problem enriches the possible physical applications.

We consider a particle moving in a one-dimensional potential. Then the Siegert pseudostates are defined by:

$$\left(\hat{H} - E\right) \phi(x) = 0, \qquad \hat{H} = -\frac{1}{2}\frac{d^2}{dx^2} + \hat{V}(x), \qquad E = \frac{1}{2}k^2 \tag{3.41}$$

with boundary conditions

$$\left(\frac{d}{dx} + ik\right) \phi(x)\bigg|_{x=-a} = 0 \tag{3.42}$$

$$\left(\frac{d}{dx} - ik\right) \phi(x)\bigg|_{x=a} = 0 \tag{3.43}$$

Since the interval of our interest is $[-a, a]$, for the numerical treatment, instead of r we introduce a new variable x, such that

$$r = ax \tag{3.44}$$

Then the interval $r \in [-a, a]$ maps onto $x \in [-1, 1]$, and the basis defined by Legendre polynomial can be utilized. We expand the solutions of Eq.(3.45) in terms of the DVR basis

$$\phi(x) = \sum_{j=1}^{N} c_j \pi_j(x) \qquad -1 \leq x \leq 1 \tag{3.45}$$

Substituting this into Eq.(3.45), premultiplying by $\pi_i(x)$ and integrating over $x \in [-1, 1]$, and using the boundary conditions, Eq.(3.46) and Eq.(3.47), we arrive at the algebric eigenvalue problem

$$\left(\tilde{\mathbf{H}} - \frac{ik}{2}\mathbf{L} - \frac{k^2}{2}I\right) \mathbf{c} = 0 \tag{3.46}$$

here **c** denotes vector of coefficients matrix and boldface characters represent matrix representation in DVR basis. I is identity matrix of size $N \times N$. Here the matrix elements are given by

$$\tilde{H}_{ij} = \frac{2}{a}\tilde{K}_{ij} + \frac{a}{2}V(x_i)\delta_{ij} \tag{3.47}$$

$$\tilde{K}_{ij} = \frac{1}{2}\int_{-1}^{1} \frac{d\pi_i(r)}{dr}\frac{d\pi_j(r)}{dr}dr \tag{3.48}$$

$$L_{ij} = \pi_i(a)\pi_j(a) + \pi_i(-a)\pi_j(-a) \tag{3.49}$$

Poltential matrix is diagonal in DVR basis and x_i are quadrature abscissas of Legnedre polynomials. Calculation of matrix elements $\tilde{K}_{ij}$ and L_{ij} are calculated in Legendre FBR basis and then transformed by transformation matrix **T**. For $\tilde{\mathbf{K}}$ we have

$$\tilde{\mathbf{K}} = \mathbf{T}^T\tilde{\mathbf{K}}^{FBR}\mathbf{T} \tag{3.50}$$

where

$$\tilde{K}_{nm} = K^{\varphi}_{nm} = \frac{1}{2}\varphi_n(1)\varphi_m(1)\left(\left\lfloor\frac{m-2}{2}\right\rfloor + 1\right)\left(2m - 2\left\lfloor\frac{m-2}{2}\right\rfloor - 1\right) \tag{3.51}$$

for $n \geq m$ and $n, m = 1, 2, 3, ...$ and $K^{\varphi}_{mn} = K^{\varphi}_{nm}$
And the matrix elements of **L**

$$\mathbf{L} = \mathbf{T}^T\mathbf{L}^{FBR}\mathbf{T} \tag{3.52}$$

where

$$L^{FBR}_{ij} = \varphi_n(1)\varphi_n(1) + \varphi_n(-1)\varphi_n(-1) \tag{3.53}$$

Now we have differential equation in algebraic form and we can easily compare this with general quadratic equation

$$\left(\mathbf{A} + \lambda\mathbf{B} + \lambda^2\mathbf{I}\right)\mathbf{c} = 0 \tag{3.54}$$

$$\mathbf{A} = 2\tilde{\mathbf{H}}, \qquad \mathbf{B} = -\mathbf{L}, \qquad \lambda = ik \tag{3.55}$$

Again the matrix **A** and **B** are real and symmetric.

3.7 Model problems

3.7.1 Smooth barrier potential

Here we consider the potential

$$V(x) = (0.5x^2 - 0.8)e^{-0.1x}, \qquad -\infty \leq x \leq \infty \tag{3.56}$$

which is full axis version of potential(3.41). In this potential there one bound state five resonant states in which three are highly converged.

Analysis of results from this potential is similar to the previous ones as Fig.3.7(a) and 3.7(b) depict eigenvalues in complex k and energy plane respectively, and in 3.7(c) potential(3.57) with resonance state wavefunctions are plotted.

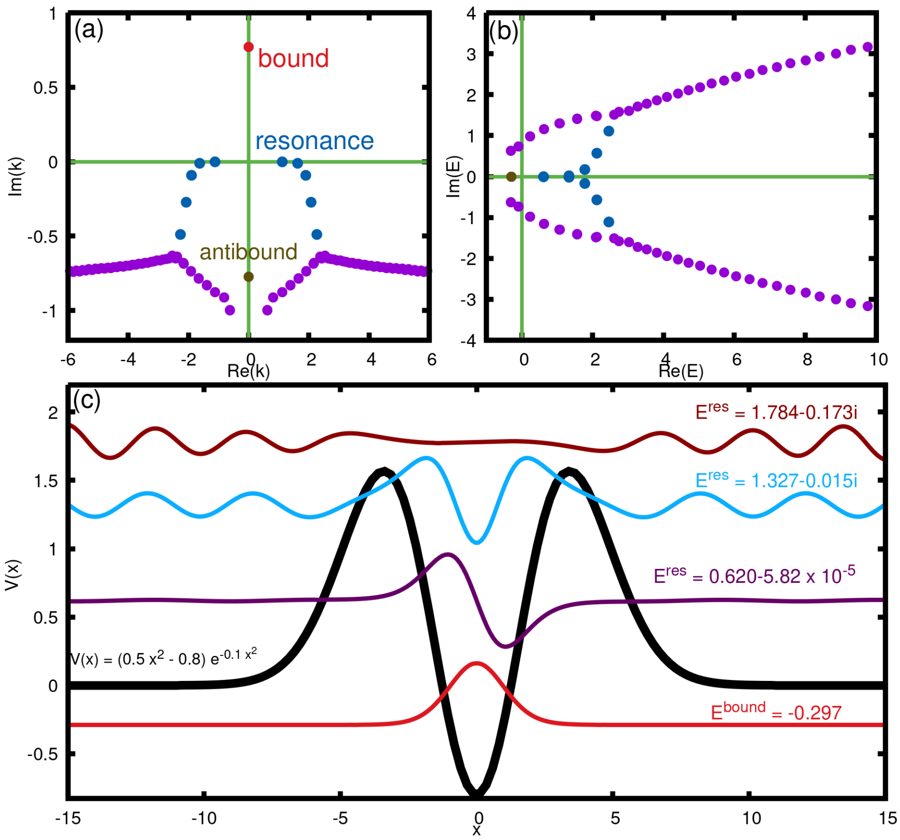

Fig. 3.7.: SPS eigenvalues and wavefunction plots for potential(3.57) with cutoff length $a = 25$, calculated using $N = 400$ basis functions. (a) Complex$-k$ distribution. (b) Complex energy distribution. (c)Potential with wavefuctions of resonance states.

3.7.2 Rectangular double barrier

The model considered previously has smooth barrier with decaying nature. Here we discuss a potential which is a rectangular double barrier given by

$$V(x) = \begin{cases} V_0, & \text{for } -1.5 \leq n \leq -0.5 \\ V_0, & \text{for } 0.5 \leq n \leq 1.5 \\ 0, & \text{for otherwise} \end{cases} \tag{3.57}$$

Here the maximum height of barrier V_0 is 10. This potential has many resonance states but only two of them are converged upto two digit accuracy. Slow convergence of the eigenvalues in this potential can be understood by derivative discontinuity of this potential.

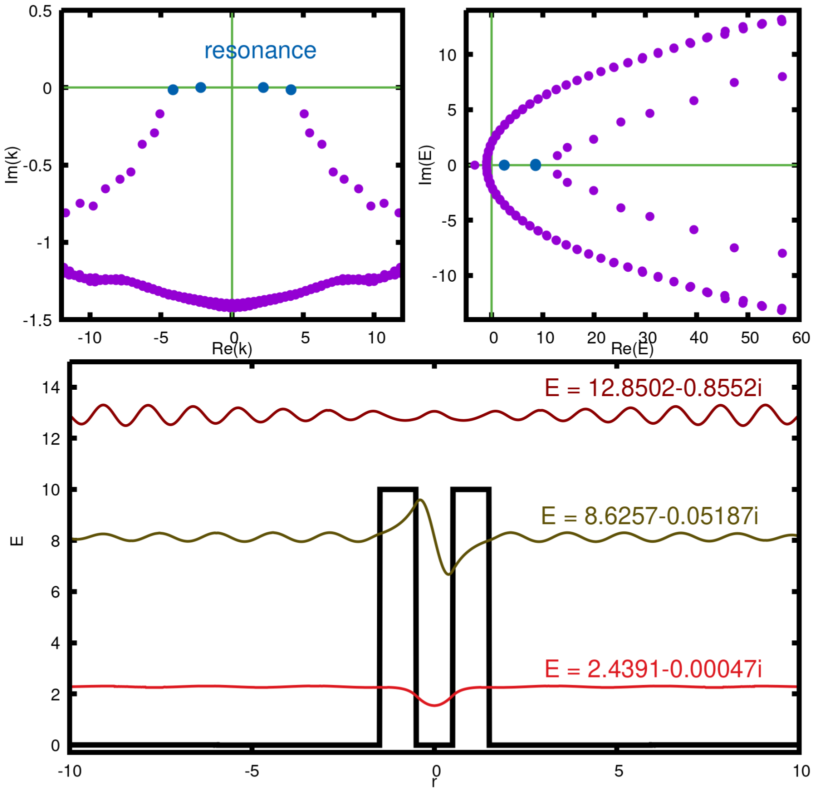

Fig. 3.8.: SPS eigenvalues and wavefunction plots for potential(3.58) with cutoff length $a = 10$, calculated using $N = 400$ basis functions. (a) Complex-k distribution. (b) Complex energy distribution. (c)Potential with wavefuctions of resonance states.

In Fig. 3.8(a) and 3.8(b), eigenvalues of SPS are plotted in complex k plane and energy plane, respectively. Potential with wavefunctions for three resonant states are plotted in Fig. 3.8(c).

Despite of slow convergence of SPSs compared to smooth potentials the eigenvalues start converging with increment of basis size N . In Fig. 3.9 complex k eigenvalues are depicted for different basis size. As can be seen for small basis size N = 100 lower eigenvalues are chaotic but when basis size reaches 600 they arrange in nice shape and start converging, though convergence in not very fast

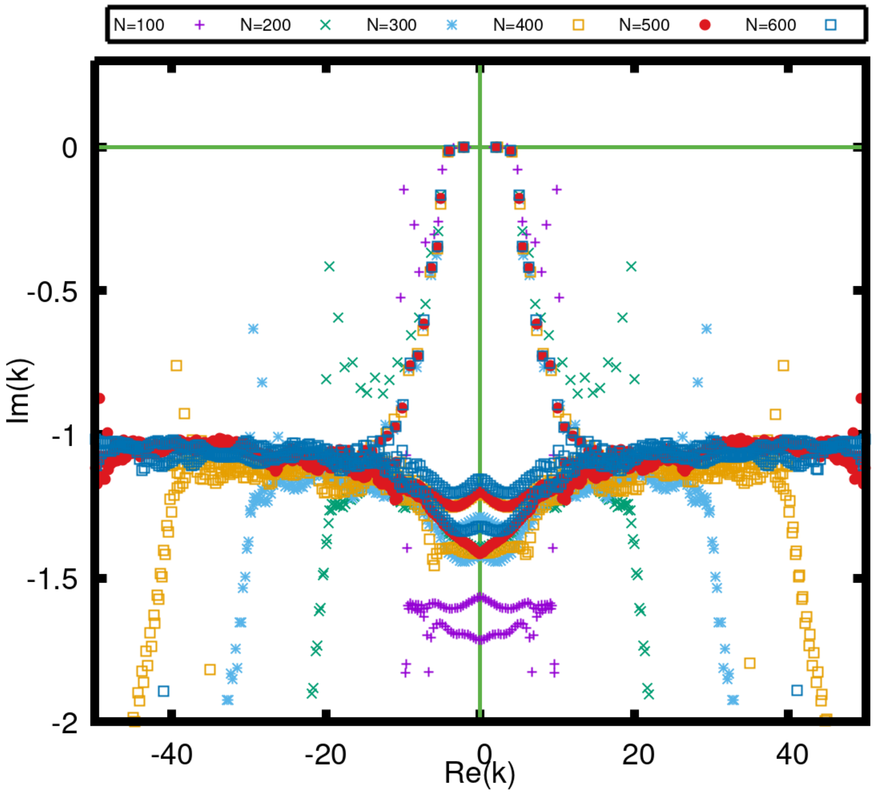

Fig. 3.9.: Complex k eigenvalues for rectangular double barrier (3.58) for different basis size N

3.8 Conclusion

Siegert pseudostates method provides a numerical tool to implement the power of Siegert states as a universal tool that is capable of treating the whole spectrum of collision phenomena. The numerical efficiency of the method is demonstrated by a number of model problems.

The universality of the SPS method can be viewed from the perspective that it treats bound states, antibound states, resonance states, and continuum in a single calculation. In comparison to the complex scaling method, it does not require an analytical continuation of potential energy in the complex r plane. In contrast to the stabilization method, it yields resonance position and width directly without any fitting procedure.

Bibliography

[1] J. C. Light, I. P. Hamilton, and J. V. Lill, J. Chem. Phys. **82**, 1400 (1985).

[2] M. Abramowitz and I. A. Stegun, editors, *Handbook of Mathematical Functions* (Dover, New York, 1972), Chapter 22.

[3] D. O. Harris, G. G. Engerholm, and W. D. Gwinn, **43**, 1515 (1965); ibid. **49**, 4209 (1968).

[4] A. J. F. Siegert, Phys. Rev. **56**, 750 (1939).

[5] O. I. Tolstikhin, V. N. Ostrovsky, and H. Nakamura, Phys. Rev. Lett. **79**, 2026 (1997).

[6] O. I. Tolstikhin, V. N. Ostrovsky, and H. Nakamura, Phys. Rev. A **58**, 2077 (1998).

[7] H. J. Korsch, R. Möhlenkamp, and H.-D. Meyer, J. Phys. B 17, 2955 (1984).

[8] Calculations Done by Prashant(prashantsingh.1993@gmail.com)

[9] Nimrod Moiseyev, *Non-Hermitian Quantum Mechanics* (Cambridge University Press, 2011) p. 8

4 Wigner and Husimi distributions for Siegert pseudostates

> *Innovation distinguishes between a leader and a follower.*
>
> — **Steve Jobs**
> (CEO Apple Inc.)

Classical mechanics gives very good description of nature. In this mechanical system is described by a Hamiltonian function $H(x, p, t)$. In classical case the state of a system which has $n-$degree of freedom can be described by a point in $2n$ dimensional phase space $(x_1, x_2, x_3...x_N; p_1, p_2, p_3...p_N)$. If we measure a system at a certain point of time we can find it at position $(x(t), p(t))$ in phase space with unit probability.

In quantum mechanics, such measurements cannot be done to describe the classical trajectory of the system. This limitation arises due to the Heisenberg uncertainty principle[1], which states that it is impossible to ascertain the system's position in phase space. Instead, we say that for a system with n degree of freedom, the system is in a volume of order h^n. Here h is plank's constant. Phase space formulation of quantum mechanics started with the contribution of Wigner[2], and many others. Similar to the Hamiltonian mechanics, in phase space, position and momentum are treated equally. Phase space description allows us to understand the quantum system's knowledge by comparing it with classical systems.

In this chapter, we focus on Wigner and Husimi[3] distributions. In phase space context, the Wigner distribution function, introduced by Eugene Wigner in 1932, acquires paramount significance. This function has been used in many areas of science such as quantum chemistry, statistical mechanics, quantum optics, and many other engineering fields. Every quantum state can be represented in terms of the Wigner function. This function can have negative value regions, which makes its probabilistic description questionable. The problem of negativity can be overcome by Husimi or Q-distribution, introduced by Husimi, which is another useful tool.

4.0.1 Winger and Husimi functions:

In 1932 Wigner proposed a distribution, known as Wigner quasiprobability distribution, to link wavefunction in position space to a probability distribution in momentum-position phase space. The formula for Wigner function of a one dimensional wavepacket $|\psi\rangle$ is given by[6]

$$W_f(x,p) = \frac{1}{2\pi\hbar}\int_{-\infty}^{\infty} \psi^*\left(x+\frac{s}{2}\right)\psi\left(x+\frac{s}{2}\right)e^{\frac{i}{\hbar}ps}ds \tag{4.1}$$

This formula can be understood as a Fourier transform of convolution of the wavepacket. Wigner function can take negative values, so it cannot be interpreted as a simultaneous probability distribution, and quasiprobability is a better term for this. For a normalized wavepacket $|\psi\rangle$ Wigher function satisfies normalization condition.

$$\int_{-\infty}^{\infty}\int_{-\infty}^{\infty} W_f(x,p)dxdp = 1 \tag{4.2}$$

Wigher function is a real function. It can be understood from Eq.(4.1), that complex conjugate of Wigner function is same function.

$$W_f(x,p) = (W_f(x,p))^* \tag{4.3}$$

If wigner function $W_f(x,p)$ is integrated over momentum p then it gives probability in position space x.

$$|\psi(x)|^2 = \int_{-\infty}^{\infty} W_f(x,p)dp \tag{4.4}$$

Similarly, if $W_f(x,p)$ is integrated over position it gives probability in momentum space.

$$\left|\tilde{\psi}(p)\right|^2 = \int_{-\infty}^{\infty} W_f(x,p)dx \tag{4.5}$$

Where $\tilde{\psi}$ is wavefunction in momentum space derived from $\psi(x)$ by fourier transform

$$\tilde{\psi}(p) = \frac{1}{\sqrt{\pi}}\int_{-\infty}^{\infty} e^{-ipx}\psi(x)dx \tag{4.6}$$

Eq.(4.4) and Eq. (4.5) show that the Wigner function has some desirable analytical properties. For its projection in both position and momentum space gives the correct quantum and position distribution.

Despite being a very useful function, the Wigner function exhibits oscillations that often go into ranges of negative values. This behavior of the Wigner function is not acceptable for a probability distribution function. Another distribution function proposed by Husimi in 1940, called Husimi distribution, is a smooth version of the Wigner function. Husimi function is obtained by smoothing negative regions of Wigner function by averaging over a coarse-graining Gaussian function[7]

$$H_f(x,p) = \int_{-\infty}^{\infty}\int_{-\infty}^{\infty} W_f(x',p')f(x,p;x',p')dx'dp' \tag{4.7}$$

The Gaussian function, $f(x,p;x',p')$, is given by,

$$f(x,p;x',p') = \frac{1}{\sqrt{\pi\hbar}}\exp\left(-\frac{\frac{(x-x')^2}{\sigma_q^2}+\sigma_q^2(p-p')^2}{\hbar}\right) \tag{4.8}$$

Here σ_q is a parameter for the width of Gaussian. This parameter determines relative resolution in position and momentum space and can be chosen freely. Husimi function is non-negative everywhere and properly normalized.

$$\int_{-\infty}^{\infty}\int_{-\infty}^{\infty} H_f(x,p)dxdp = 1 \tag{4.9}$$

therefore, it can be interpreted as a genuine distribution of probability. In comparison with the Wigner function, Husimi function does not recover observabales, which are obtained for Wigner case as defined in Eq. (4.4), (4.5). for Wigner function.

4.1 Numerical Implementation

For an analytical and localized wavepacket, Wigner and Husimi distribution functions can be calculated using the formula Eq.(4.1) and Eq.(4.47). The integration can be calculated by analytical or any numerical method such as Gaussian quadrature method. To calculate these functions for a discrete and diverging wavepacket, some special numerical techniques are used.

Siegert pseudostates calculation for potential, Eq. (3.57), was calculated by the numerical procedure given in Chapter 3. Since the eigenvectors obtained from SPS calculations are discrete points, we utilized interpolation method to calculate the wavefunction at any point in the interval $[-a,a]$. General wavefunction can be calculated by SPS eigenvectors in the region $[-a, a]$ and by boundary conditions, Eq. (3.42), (3.43) in the outside region.

$$\psi(x) = \begin{cases} = Ae^{ikx} & \text{if } x < -a \\ = \psi^{SPS}(x) & \text{if } -a \geq x \leq a \\ = Be^{ikx} & \text{if } x > a \end{cases} \tag{4.10}$$

Here A and B are some complex constants. These constants can be calculated by the fact that wavefunction is continuous. $\psi^{SPS}(x)$ is wavepacket obtained by interpolation of eigenvectors.

$$\psi^{SPS}(-a) = Ae^{-ika} \quad \text{and} \quad \psi^{SPS}(a) = Ae^{ika} \tag{4.11}$$

Now we have a general formula, Eq. (4.9), for SPS eigenvectors in $(-\infty, \infty)$ interval. We can calculate the Wigner and Husimi distribution using the formula in Eq.(4.1) and Eq. (4.47), but the interval of integration has to be chosen a finite range.

$$W_f(x,p) = \int_{-S}^{S} \psi^* \left(x + \frac{s}{2}\right) \psi \left(x + \frac{s}{2}\right) e^{\frac{i}{\hbar}ps} ds \tag{4.12}$$

The normalization constant N^{RES} was calculated by considering some predecided value of integral limits in position

$$N_{RES}^2 \int_{-a}^{a} |\psi(q)|^2 \, dq = 1 \tag{4.13}$$

4.2 Results and discussion

4.2.1 Interference in wavepacket constructed from a superposition of two Gaussian functions

Before going into resonance states of the SPS method, we introduce a model example of a wavefunction with probability density at two different centers. This wavefunction is constructed by taking two Gaussian functions at two difference centers, shown in Fig. (4.1). Momentum space wavefunction $\tilde{\psi(p)}$ is also calculated by Eq. (4.6). When the wavefunction is a Gaussian the momentum wavefunction is also Gaussian. However, for the wavefunctions with probability density separated the momentum wavefunction gets negative and positive values. The importance of

Wigner function is that we can visualize both position x and momentum p probabilities in single distribution. In Figure (4.2) the Wigner distribution and Husimi

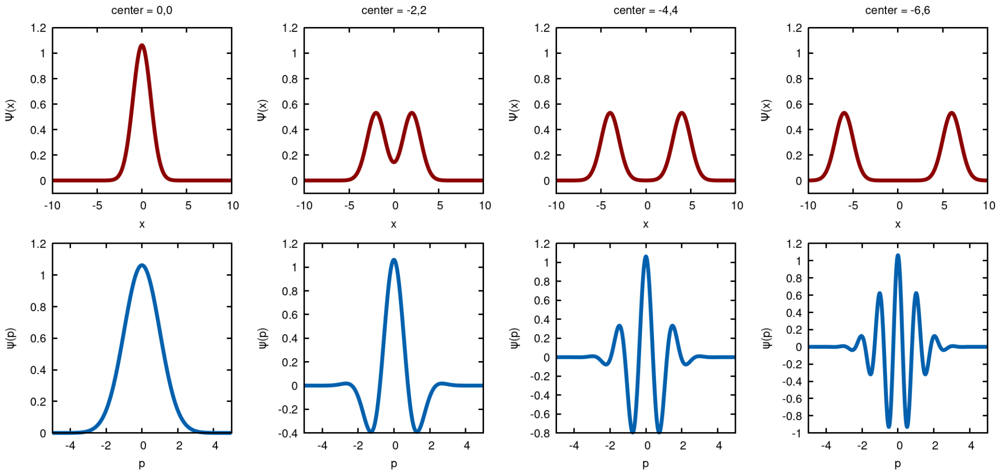

Fig. 4.1.: Wavefunction constructed by combination of two Gaussians in position space(first row) and in momentum space(second row)

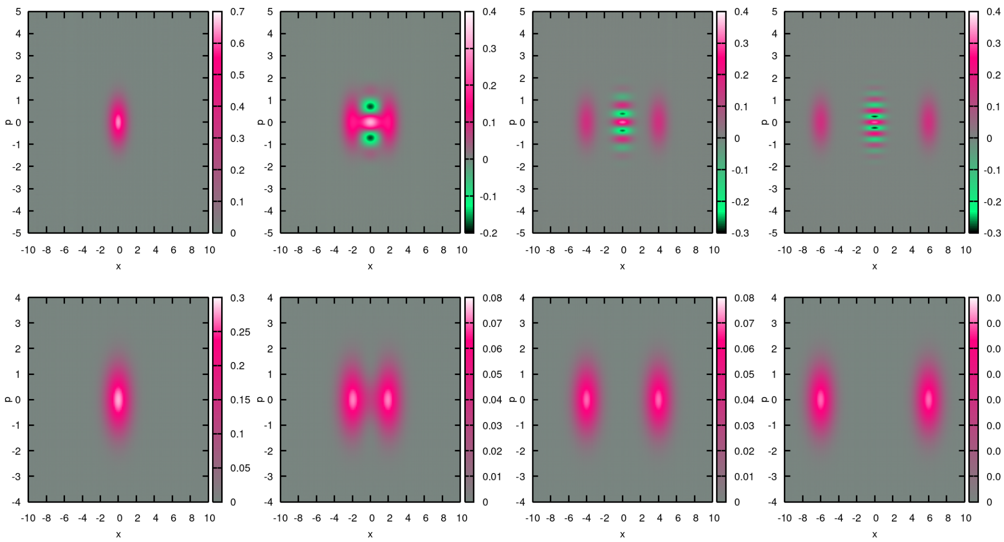

Fig. 4.2.: Wigner distribution(first row) and Husimi distribution (second row) for wavefunctions in Fig. (4.1)

distributions are depicted. For the case of single Gaussian wavefunction the Wigner distribution is also a Gaussian in two dimension. However, when the centers of two Gaussian separate we start getting some regions with negative probability. When the Gaussians are completely separated from each other some fringe like structure appear in the middle of two centers. These fringes appear due to the interference of the two Gaussians. It can be seen that the fringes of an interference pattern remain aligned with the straight line joining the two centers. An increase/decrease in the distance between two Gaussian centers leads to the decrease/increase in the transverse spacing of the fringes. The negative regions of Wigner distribution indicate a quantum mechanical phenomenon.

The negative regions of Wigner can be removed by "coarse graining", and we get the Husimi distribution which is positive everywhere. The smoothing of Wigner distribution results in the spread of probability and hence the Husimi distribution does not provide correct probabilities.

4.2.2 Tunneling of resonances states of a smooth double barrier potential

By choosing a basis size of $N = 300$ and cutoff length of $a = 15$ we get $2N = 600$ eigenvalues and corresponding eigenvectors. Values of momentum and and energy are calculated using relations $\lambda = ik$ and $E = \frac{1}{2}k^2$. All energy eigenvalue except bound and antibound states are complex, and those values which lie very close to the real energy axis correspond to resonance states. The resonance eigenvalues and eigenvectors are depicted in Figure. (4.1). There are two resonance states which lie above the threshold level and below the maximum of the barrier.

From the position of complex k values in the $k-$plane and Eq.(4.9), we can understand that for large value of x wavefunction decays exponentially. However, for antibound(virtual) states, wavefunction grows exponentially, and these wavefunctions do not have oscillatory behavior. The wavefunction of a resonance state always grows exponentially with x. Growing and decaying resonance wavefunction have the same shape but have oscillatory behavior in the non-interaction region with only difference in phase of oscillations. Resonance states lying below the maximum height of the barrier are quasistationary. In these states, particles can escape into the outer region by tunneling, which is an entirely quantum mechanical phenomenon.

From now on, we will call resonance of lower energy, $E^{RES} = 0.620$, as first resonance and resonance with higher energy, $E^{RES} = 1.327$, as second resonance.

Figure. (4.4) shows the Wigner distribution for bound and antibound states. Bound state Wigner distribution is Gaussian shaped but for the antibound state it is Gaussian shaped. The reason behind it is that in interaction region bound and antibound states are almost same with only a difference in phase.

Figure. (4.4) shows the Wigner distribution functions for first and second resonance. Due to lower energy, resonance tunneling in the first resonance is very weak. This

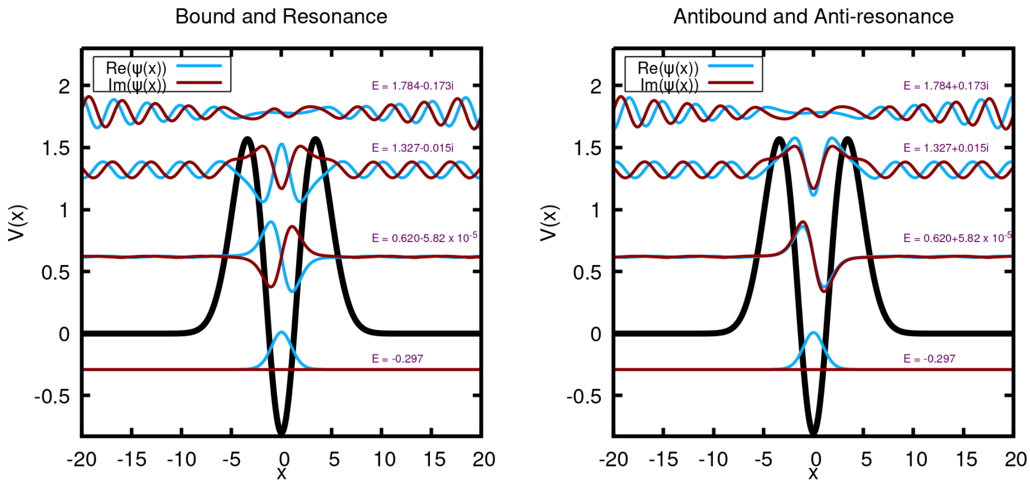

Fig. 4.3.: Siegert pseudostates wavefunctions for bound, antibound, resonance and antiresonance states of potential (3.57)

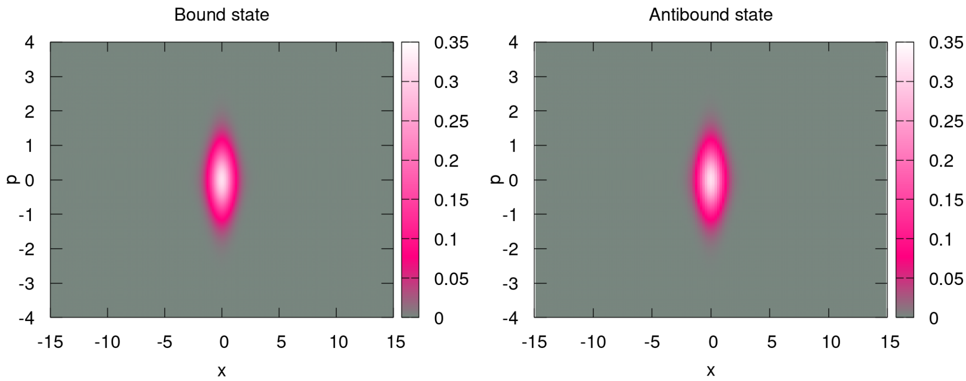

Fig. 4.4.: Wigner distribution for bound and antibound states in Figure. (4.3)

can be understood from the Wigner distribution as interference patterns are faded in the outer region, and most of the population lies in the interaction region. However, due to higher energy, tunneling through the barrier is very profound in second resonance. Wigner distribution for second resonance shows a highly intense interference pattern.

For the large positive value of x, the Wigner function tends towards positive momentum, and for a large negative value of x, it goes towards negative momentum value. This behavior shows that resonance decaying from the interaction region and going towards a potential free region. For antiresonance states, this tendency is quite the opposite which shows their growing nature, Figure. (4.5). The Wigner function in the interaction region always remains the same as the normalization is a constant

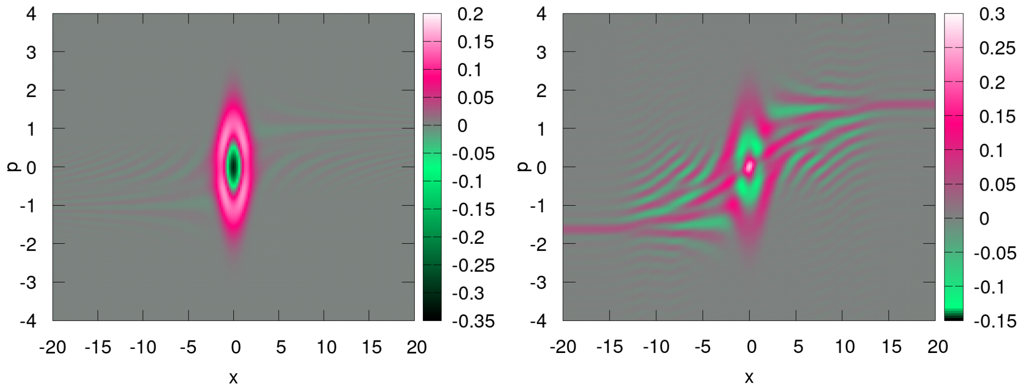

Fig. 4.5.: Wigner distribution for first and second resonance states in Figure. (4.3)

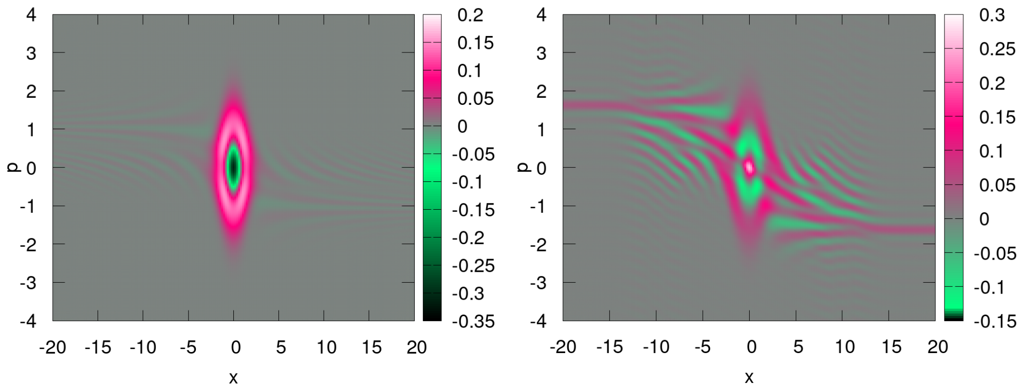

Fig. 4.6.: Wigner distribution for first and second anti-resonance states in Figure.(4.1)

value. Diverging nature of the wavepacket does not affect the Wigher function close to the interaction region.

Tab. 4.1.: Normalization value of First and Second resonance wigner distribution for different range of integration in Eq.(4.1)

S	First resonance	Second resonance
40	1.000478	0.999926
50	1.000505	1.000294
60	1.000505	1.000409
70	1.000505	1.000606
80	1.000505	0.999555

Negative regions that appeared in the Wigner distribution make it less relevant to consider as a probability density. However, Husimi distribution, which is mathematically described in previous sections, is smoothed version of the Wigner function. As depicted in Figure. (4.5), Husimi distribution is a positive distribution that is more

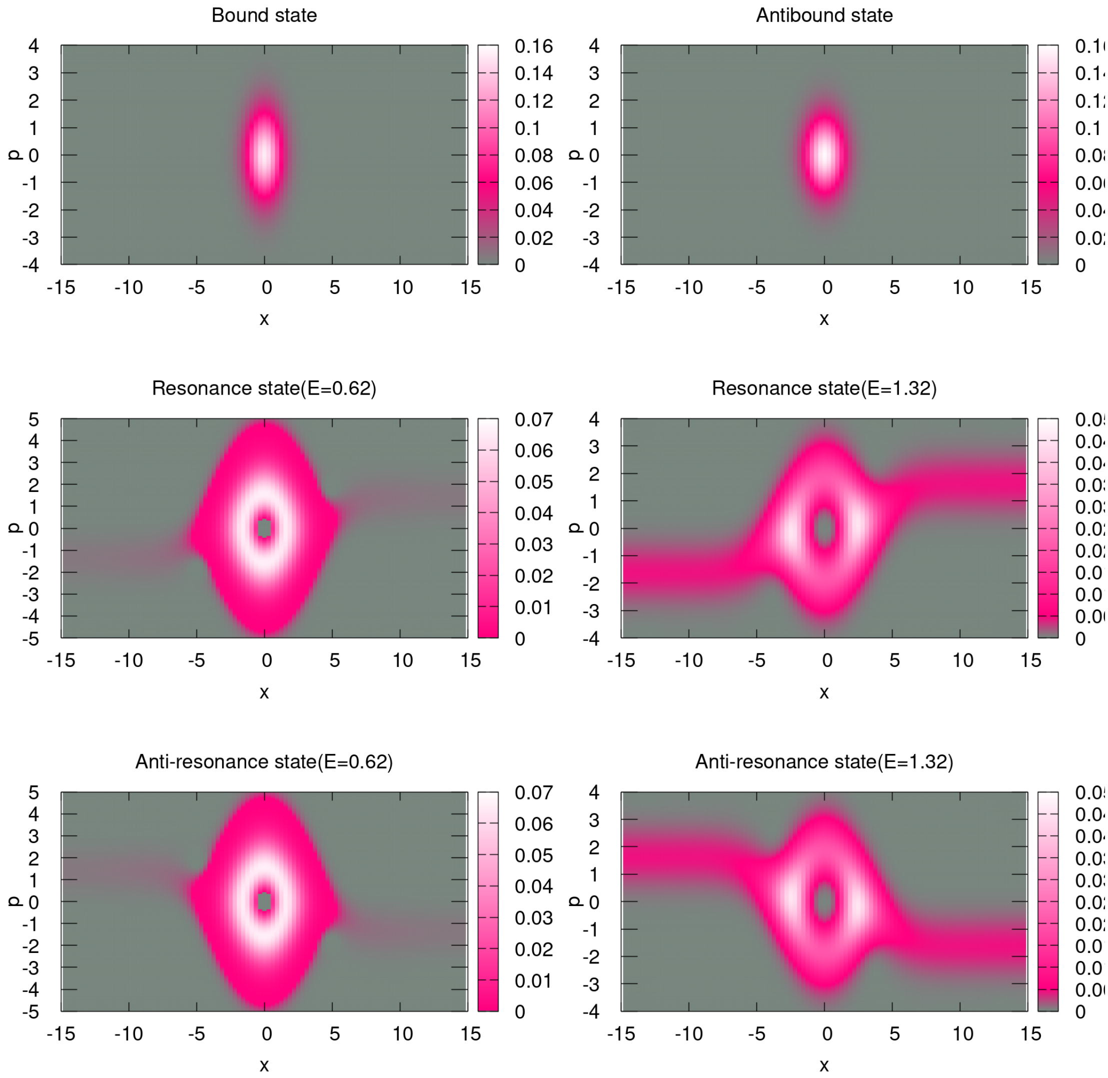

Fig. 4.7.: Husimi distribution for the Siegert pseudostates in Figure.(4.3) calculated with $\sigma_q = 1$

relevant to classical distribution. Despite the non-negativity of Husimi distribution, it does not follow relations like Eq.(4.4) and Eq.(4.5).

4.3 Conclusion

Phase space representation for classical system describes all possible states of the system. However, due to the uncertainty principle, quantum systems are described by probability density. The Wigner distribution approach provides a good description of the system as a quasi probability. The negative regions of Wigner functions are due to the quantum mechanical phenomenon and fade away after smoothing the function with a Gaussian function. Resonance tunneling of the resonance Siegert pseudostates is described very well with the Wigner distribution by depicting interference patterns. One of the important use of these phase space representations is that these Wigner and Husimi distributions can distinguish between resonance and anti-resonance states.

Bibliography

[1] W. Heisenberg, Z. Phys. **33**, 879 (1925)

[2] E. P. Wigner, Phys. Rev. **40**, 749 (1932).

[3] K. Husimi, Proc. Phys.-Math. Soc. Jpn. **22** , 264 (1940).

[4] K. Takahashi, J. Phys. Soc. Jpn. **55** , 762 (1986).

[5] Naomichi Hatano, Keita Sasada, Hiroaki Nakamura and Tomio Petrosky, Progress of Theoretical Physics, Vol. 119, No. 2, February 2008

[6] *Quantum Evolution: An Introduction to Time-Dependent Quantum Mechanics*, by James E. Bayfield(1999), Wiley-VCH,p.29.

[7] *Introduction to Quantum Mechanics* by David J. Tannor(2007),University Science Books,p.58

[8] A. J. F. Siegert, Phys. Rev. **56**, 750 (1939).

[9] O. I. Tolstikhin, V. N. Ostrovsky, and H. Nakamura, Phys. Rev. Lett. **79**, 2026 (1997).

[10] O. I. Tolstikhin, V. N. Ostrovsky, and H. Nakamura, Phys. Rev. A **58**, 2077 (1998).

List of Figures

List of Tables

List of Listings

Appendix A

A.1 Evaluation of $\tilde{\mathbf{K}}^{FBR}$

The matrix elements of $\tilde{\mathbf{K}}^{FBR}$ are representation in finite normalized basis which is constructed from Legendre polynomials

$$\begin{aligned}\tilde{K}^{FBR}_{nm} &= \frac{1}{2}\int_{-1}^{1}\frac{d\varphi_n(x)}{dx}\frac{d\varphi_m(x)}{dx}dx\\ &= \frac{1}{2}\frac{1}{\sqrt{h_{n-1}h_{m-1}}}\int_{-1}^{1}\frac{dP_{n-1}(x)}{dx}\frac{dP_{m-1}(x)}{dx}dx\\ &= \frac{1}{2}\frac{1}{\sqrt{h_{n-1}h_{m-1}}}\int_{-1}^{1}\frac{dP_{n-1}(x)}{dx}\frac{dP_{m-1}(x)}{dx}dx\end{aligned} \tag{A.1}$$

Here h_n is given by

$$h_n = \frac{2}{2n+1}$$

Derivative of Legendre polynomial can be expanded in terms of Legendre polynomials

$$\frac{d}{dx}P_{n+1}(x) = (2n+1)P_n(x) + (2(n-2)+1)P_{n-2}(x) + (2(n-4)+1)P_{n-4}(x) + \cdots$$

$$\frac{d}{dx}P_{n+1}(x) = \sum_{\substack{k=0\\k=even}}^{n}\left[2(n-k)+1\right]P_{n-k}(x), \tag{A.2}$$

then

$$\begin{aligned}\int_{-1}^{1}\frac{dP_{n+1}(x)}{dx}\frac{dP_{m+1}(x)}{dx}dx &= = \sum_{\substack{l,k=0\\l,k=even}}^{k=n,l=m}\left[\left[2(n-k)+1\right]\left[2(m-l)+1\right]\int_{-1}^{1}P_{n-k}(x)P_{m-l}(x)dx\right]\\ &= \sum_{\substack{k,l=0\\k,l=even}}^{k=n,l=m}\left[\left[2(n-k)+1\right]\left[2(m-l)+1\right]\frac{2\delta_{n-k,m-l}}{\left[2(n-k)+1\right]}\right]\end{aligned}$$

In above summation the therms with $n-k=m-l$ will survive and we arrive at condition

$$\int_{-1}^{1}\frac{dP_{n+1}(x)}{dx}\frac{dP_{m+1}(x)}{dx}dx=\sum_{\substack{l=0\\l=even}}^{m}2\left[2(m-l)+1\right],\qquad \text{for } n\geq m \quad \text{and } n,m=0,1,2,\cdots$$
$$=\left(\left[\frac{m}{2}\right]+1\right)\left(2m-2\left[\frac{m}{2}\right]+1\right)$$

where [.] denotes greatest integer function

then

$$K_{nm}^{FBR}=\frac{1}{2}\frac{1}{\sqrt{h_{n-1}h_{m-1}}}\left(\left[\frac{m-2}{2}\right]+1\right)\left(2m-2\left[\frac{m-2}{2}\right]-1\right) \tag{A.3}$$

for $n\geq m$ and $n,m=1,2,3,\cdots$ and $K_{mn}^{(\varphi)}=K_{nm}^{(\varphi)}$

A.2 Matrix elements for full axis problems

Here we elaborate the algebra used to calculate matrix elements for generalized eigenvalue problem. To achieve Eq.(3.48),(3.49),(3.50) we consider the one dimensional schrödinger equation

$$\left(-\frac{1}{2}\frac{d^2}{dr^2}+V(r)-E\right)\phi(r)=0 \tag{A.4}$$

pre multiplication with $\pi_i(r)$ and integrate

$$\left[-\frac{1}{2}\int_{-a}^{a}\pi_i(r)\frac{d}{dr}\left(\frac{d\phi(r)}{dr}dr\right)+\int_{-a}^{a}\pi_i(r)V(r)\phi(r)dr\right.$$
$$\left.-E\int_{-a}^{a}\pi_i(r)\phi(r)dr\right]=0$$

integrating first term by parts

$$\left[\left(-\frac{1}{2}\pi_i(r)\frac{d\phi(r)}{dr}\right)_{-a}^{a}+\frac{1}{2}\int_{-a}^{a}\frac{d\pi_i(r)}{dr}\frac{d\phi(r)}{dr}dr+\int_{-a}^{a}\pi_i(r)V(r)\phi(r)dr\right.$$
$$\left.-E\int_{-a}^{a}\pi_i(r)\phi(r)dr\right]=0$$

Applying boundary conditions in first term

$$\Big[-\frac{ik}{2}\pi_i(a)\phi(a) - \frac{ik}{2}\pi_i(-a)\phi(-a) + \frac{1}{2}\int_{-a}^{a}\frac{d\pi_i(r)}{dr}\frac{d\phi(r)}{dr}dr + \int_{-a}^{a}\pi_i(r)V(r)\phi(r)dr - \frac{k^2}{2}\int_{-a}^{a}\pi_i(r)\phi(r)dr\Big] = 0$$

then by expanding $\phi(r)$ in terms of basis functions

$$\phi(r) = \sum_{j=1}^{N}\vec{c}_j\pi_j(r) \quad \text{(A.5)}$$

$$\sum\Big[-\frac{ik}{2}\pi_i(a)\pi_j(a) - \frac{ik}{2}\pi_i(-a)\pi_j(-a) + \frac{1}{2}\int_{-a}^{a}\frac{d\pi_i(r)}{dr}\frac{d\pi_j(r)}{dr}dr + \int_{-a}^{a}\pi_i(r)V(r)\pi_j(r)dr - \frac{k^2}{2}\int_{-a}^{a}\pi_i(r)\pi_j(r)dr\Big]\vec{c}_j = 0$$

$$H_{ij} = \frac{1}{2}\int_{-a}^{a}\frac{d\pi_i(r)}{dr}\frac{d\pi_j(r)}{dr}dr + \int_{-a}^{a}\pi_i(r)V(r)\pi_j(r)dr = 0$$

$$L_{ij} = \pi_i(a)\pi_j(a) + \pi_i(-a)\pi_j(-a)$$

Appendix B

B.1 Codes

All the codes related to this work are written in Fortran90 programming language.

B.2 Compiler and Packages Used

gfortran (GNU Fortran Version-9.3.0)
Copyright (C) 2019 Free Software Foundation, Inc.

B.3 Packages Used

LAPACK(Linear Algegra PACKage) to call subroutine "dsyev" and "zgeev".

B.4 Compilation of code

Bash command to compile the code

```
$ gfortran siegert_code.f90 siegert_subroutine.f90
  -llapack -lblas -o output.exe
```

Listing B.1: Compiling fortran code in Bash terminal

B.5 Codes and Subroutines

```
! siegert_code.f90
! Module named param used to store parameters
  module param
  implicit none
   real*8, parameter :: zero = 0.00000d+00
   real*8, parameter :: half = 0.500000d+00
   real*8, parameter :: one  = 1.00000d+00
   real*8, parameter :: two = 2.0000000d+00
   real*8, parameter :: pi = 3.1415926535
   complex*16, parameter :: cone = (one, zero)
   complex*16, parameter :: zi = (zero, one)
   complex*16, parameter :: czero =(zero,zero)
  end
! Main program starts Here
  program outgoingdvr
  use param
  implicit none
  real*8, allocatable :: absi(:), wt(:)
  real*8, allocatable :: poly(:,:), phi(:,:), norm(:)
  real*8, allocatable :: t(:,:)
  real*8, allocatable :: kphi(:,:),kmat(:,:)
  real*8, allocatable :: rho(:,:),umat(:,:), matl(:,:)
  real*8, allocatable :: a(:,:), b(:,:), hmat(:,:),identity(:,:)
  real*8, allocatable :: rhohalf(:,:), rhovec(:,:), rhoeval(:)
  real*8, allocatable :: rhodiag(:,:)
  real*8, allocatable :: amatrix(:,:), bmatrix(:,:)
  real*8, allocatable :: bevec(:,:), ddiag(:)
  complex*16, allocatable :: utilde(:,:), utilded(:,:)
  complex*16, allocatable :: atilde(:,:)
  complex*16, allocatable :: camat(:,:)
  complex*16, allocatable :: eigval(:)
  complex*16, allocatable :: eigvals(:), vecr(:,:), vecl(:,:)
  complex*16, allocatable :: eigvecs(:,:)
  real*8 :: aval, alpha, beta, potential, rval
  integer :: i, j, k, l, ndim, ntdim, n
! Input values
  aval  =  one   ! maximum value of r
```

```
  ndim   =   300    ! number of basis used
!-----------------------------------------------------------
  ntdim =   2 * ndim
  alpha =   zero  ! parameter for jacobi polynomial(=0)
  beta  =   zero  ! parameter for jacobi polynimial(=0)
!  reading absisas and weight
! note : absisa and weight are calculated using
! fortran code seperately
   allocate(absi(ndim), wt(ndim))
   open(12,file='absisa3.txt')
   open(13,file = 'weight3.txt')
    read(12,*) absi
    read(13,*) wt
   close(12)
   close(13)
! generating polynomial at absisa
   allocate(poly(ndim,ndim))
   call eval_jacobipoly(poly, absi, ndim,  alpha, beta)
! norm factor evaluation
    allocate ( norm(ndim))
    do i = 1, ndim
     n = i-1
     norm(i) = two/(two*n+one)
    enddo
! calcualtion of phi
   allocate(phi(ndim,ndim))
   call eval_phi(phi, poly,norm,absi,ndim, alpha, beta)
! calculation of T matrix(FBR-DVR transformation)
   allocate(t(ndim,ndim))
   call eval_t(t,phi,absi,wt,ndim,beta)
! evaluation of Kphi(K-matrix in FBR)
   allocate(kphi(ndim,ndim))
   call eval_kphi( kphi, norm,  ndim, beta)

! evaluation of kmat(K-matrix in DVR)
   allocate( kmat(ndim,ndim))
   call dgemm ('t', 'n', ndim, ndim, ndim, one, t,  &
          ndim, kphi, ndim, zero, kmat, ndim )
   call dgemm ('n', 'n', ndim, ndim, ndim, one, kmat,&
```

```
             ndim, t, ndim, zero, kmat, ndim )
    deallocate( kphi)
! evaluation of rho matrix(DVR-Basis)
     allocate(rho(ndim,ndim))
     call eval_rho(rho, t, absi, aval, ndim, beta)
! evaluation of  potential matrix(DVR-Basis)
     allocate ( umat(ndim,ndim))
     umat = zero
     do i = 1, ndim
      rval = aval*half * ( one + absi(i))
      potential = -112.5 ! Specify Potential Here
      umat(i,i) =  potential * (rval**two)
     enddo
! evaluation of L-matrix(in DVR basis)
     allocate(matl(ndim,ndim))
     call eval_matl(matl, t, norm, beta, ndim)
! evaluation of hmat
     allocate(hmat(ndim,ndim))
     hmat = ( kmat + umat + matl )
! evaluation of rhohalf matrix
     allocate (rhohalf(ndim,ndim),  &
               rhovec(ndim, ndim), rhoeval(ndim))
     rhovec = rho
     call call_dsyev_wt_eigvecs(rhovec, ndim, rhoeval)
     allocate(rhodiag(ndim,ndim))
     rhodiag = zero
     do i = 1, ndim
      rhodiag(i,i) = one/zsqrt(cone * rhoeval(i))
     enddo
     call dgemm ('n','n',ndim,ndim,ndim,one,rhovec, ndim,&
             rhodiag, ndim, zero, rhohalf, ndim )

     call dgemm ('n','t',ndim,ndim,ndim,one,rhohalf,ndim,&
                   rhovec, ndim, zero, rhohalf, ndim )
     allocate(a(ndim,ndim),b(ndim,ndim))
     call dgemm ('n','n',ndim,ndim,ndim,two,rhohalf,ndim, &
                   hmat, ndim, zero, a, ndim )
     call dgemm ('n','n',ndim,ndim,ndim,one,a,ndim,&
                   rhohalf, ndim, zero, a, ndim)
```

```
    call dgemm ('n', 'n', ndim,ndim,ndim,-two*aval,rhohalf,&
                  ndim,matl,ndim,zero,b,ndim)
    call dgemm('n','n',ndim, ndim,ndim,one,b,ndim,&
                  rhohalf, ndim, zero, b, ndim)
    deallocate(hmat, umat, matl, rhovec, rhodiag)
! evaluation of identity matrix
    allocate(identity(ndim,ndim))
    identity = zero
    do i = 1, ndim
     identity(i,i) = one
    enddo
! evaluation of 2n x 2n matrices
     allocate( amatrix( ndim*2, ndim*2 ))
     allocate( bmatrix( ndim*2, ndim*2 ))
     do i = 1, ndim
      do j = 1, ndim
       amatrix(i,j) = -a(i,j)
       bmatrix(i,j) =  b(i,j)
      enddo
     enddo
     do i = 1, ndim
      do j = ndim + 1, 2*ndim
       k = j - ndim
       amatrix(i,j) = zero
       bmatrix(i,j) = identity(i,k)
      enddo
     enddo
     do i = ndim + 1, 2*ndim
      do j = 1, ndim
       k = i - ndim
       amatrix(i,j) = zero
       bmatrix(i,j) = identity(k,j)
      enddo
     enddo
     do i = ndim + 1, 2*ndim
      do j = ndim + 1, 2*ndim
       k = i - ndim
       l = j - ndim
       amatrix(i,j) = identity(k,l)
```

```
          bmatrix(i,j) = zero
         enddo
        enddo
       deallocate( a, b, identity)
!  solving generalized eigenvalue problem
      allocate(bevec(ntdim,ntdim), ddiag(ntdim))
      bevec = bmatrix
      call call_dsyev_wt_eigvecs(bevec, ntdim, ddiag)
      allocate( utilde(ntdim, ntdim), utilded(ntdim, ntdim))
      do i = 1, ntdim
       do j = 1, ntdim
       utilde(i,j)  =  (bevec(i,j))/( zsqrt(cone*ddiag(j)))
       utilded(i,j) =  (bevec(j,i))/( zsqrt(cone*ddiag(i)))
       enddo
      enddo
      allocate( camat(ntdim, ntdim),  atilde(ntdim, ntdim))
      camat = amatrix
      call zgemm('n', 'n', ntdim, ntdim, ntdim, cone, utilded,&
                 ntdim,camat, ntdim, czero, atilde, ntdim)
      call zgemm('n', 'n', ntdim, ntdim, ntdim, cone, atilde, &
                 ntdim, utilde, ntdim, czero, atilde, ntdim)
      deallocate(camat)
      allocate(eigvals(ntdim),vecl(ntdim,ntdim),vecr(ntdim,ntdim))

!        eigenvalue solving
      call call_zgeev_wt_eigvecs(atilde,ntdim,eigvals,vecl,vecr)

!   back transformation of eigenvectors
      allocate( eigvecs(ntdim,ntdim))
      call zgemm('n','n',ntdim,ntdim,ntdim,cone,utilde,ntdim, &
                    vecl, ntdim, czero, vecr, ntdim)
      eigvecs = matmul( rhohalf, vecr(1:ndim ,:))
      open(57, file = 'eigval.txt')
      do i = 1, ntdim
       write(57,'(*(f30.12))') -zi*eigvals(i), &
               half*(-zi*eigvals(i))**two
      enddo
      close(57)
      open(61, file = 'eigvecs.txt')
```

```
    do i = 1, ndim
     write(61,'(*(f22.12))')(aval/two)*(absi(i)+one),eigvecs(i,:)
    enddo
    close(61)
    deallocate(amatrix, bmatrix, utilde)
    deallocate(utilded, bevec, ddiag, atilde)
    deallocate(eigvals, vecl)
  end program
```

Listing B.2: Main program to evaluate Siegert pseudostates

```
! siegert_subroutine.f90
!          polynomial evaluation
subroutine eval_jacobipoly(poly, absi, ndim, alpha, beta)
  use param
  implicit none
  real(8), intent(out) :: poly(ndim,ndim)
  real(kind=8) :: eal(8), intent(in ) :: absi(ndim)
  real(8) :: alpha, beta, c1, c2, c3
  integer :: ndim, i, n
  poly(1,:) = one
  poly(2,:) = (alpha+one)+(alpha+beta+two)*(absi-one)/two
  do i=1,ndim-2
    n = i + 1
    c1 = (two*n + alpha + beta - one) * (two*n + alpha + beta)/&
         (two*n * (n + alpha + beta))
    c2 = (two*n + alpha + beta - one) * (alpha**two - beta**two)/ &
         (two*n*(n + alpha + beta) * (two*n + alpha + beta - two))
    c3 = (n + alpha - one) * (n + beta - one) * (two*n + alpha + beta
         (n*(n + alpha + beta) * (two*n + alpha + beta - two))
    poly(i+2,:) = (c1*absi + c2)*poly(i+1,:) - c3 * poly(i,:)
  enddo
end subroutine
! orthogonal phi function at absisa
subroutine eval_phi( phi, poly, norm, absis, ndim, alpha, beta)
  use param
  implicit none
  real(8) , intent(in)  :: poly(ndim,ndim),absis(ndim), norm(ndim)
  real(8) , intent(out) :: phi(ndim,ndim)
  real(8) , allocatable :: wx(:)
```

```
  integer :: ndim, n, i
  real(8) :: alpha, beta
  allocate(wx(ndim))
  wx = ((one - absis)**alpha) * ((one + absis)**beta)
  do i=1,ndim
    n=i-1
    phi(i,:) = dsqrt(wx / norm(i)) * poly(i,:)
  enddo
  deallocate(wx)
end subroutine
!   t- matrix evaluation
subroutine eval_t(t,phi,absis,wt,ndim,beta)
  use param
  implicit none
  real(8), intent(in) :: wt(ndim),absis(ndim),phi(ndim,ndim)
  real(8), intent(out):: t(ndim,ndim)
  integer :: ndim,i
  real*8  :: beta, wx
  real(8) , allocatable  :: factor(:)
  allocate(factor(ndim))
  do i = 1, ndim
    wx = (one + absis(i))**beta
    factor(i) = dsqrt( wt(i)/wx)
  enddo
  do i=1,ndim
    t(i,:) = factor*phi(i,:)
  enddo
  deallocate(factor )
end subroutine
! evaluation of kpi matrix
subroutine eval_kphi(kphi, norm, ndim, beta)
  use param
  implicit none
  real(8), intent(out)  :: kphi(ndim,ndim)
  real(8), intent(in)   :: norm(ndim)
  real(8) , allocatable :: phi1(:)
  integer :: ndim, m, n, k
  real(8) :: beta, sum1, sum2
  allocate( phi1(ndim))
```

```
  do n = 1, ndim
    phi1(n) = two**(beta/two) / dsqrt(norm(n))
  enddo
!  for diagonal terms
  sum1 = zero
  do n = 1 , ndim
    do k = 1, n -1
      sum1 = sum1 + ((phi1(k))**two)
    enddo
    kphi(n,n) = ( two * (phi1(n)**two) * sum1) + &
    half * (((phi1(n)**two) - half)**two)
    sum1 = zero
  enddo
! for off diagonal terms
  sum2 = zero
  do n = 1, ndim
    do m = n + 1, ndim
      do k = 1, n-1
        sum2 = sum2 + (phi1(k))**two
      enddo
      kphi(n,m) = phi1(n) * phi1(m) * (two * sum2 + &
      (phi1(n)**two) - half)
      kphi(m,n) = kphi(n,m)
      sum2 = zero
    enddo
  enddo
  deallocate(phi1)
end subroutine

!           evaluation of rho matrix

subroutine eval_rho(rho,t,absi,aval,ndim,beta)
  use param
  implicit none
  real(8), intent(in) :: t(ndim,ndim), absi(ndim)
  real(8), intent(out) :: rho(ndim,ndim)
  real(8), allocatable :: delta(:,:)
  real(8) :: aval,beta,dn
  integer :: ndim,i,j
```

```
  dn=(4.0*ndim**two * (ndim + beta)**two)/ &
    ((two*ndim + beta)**two * ((two*ndim+beta)**two-one))
  allocate(delta(ndim,ndim))
  delta=zero
  do i=1,ndim
    delta(i,i) = one
  enddo
  do i = 1,ndim
    do j = i ,ndim
      rho(i,j) = ((aval*half)**two) * (((one+absi(i))**two) &
           * delta(i,j) + dn * t(ndim,i)*t(ndim,j))
      rho(j,i) = rho(i,j)
    enddo
  enddo
  deallocate( delta)
end subroutine
!   lmatrix evaluation
subroutine eval_matl(matl, t, norm, beta ,ndim)
  use param
  implicit none
  real(8), intent(out) :: matl(ndim,ndim)
  real(8), intent(in)  :: t(ndim,ndim),norm(ndim)
  real(8), allocatable :: pivec(:)
  real*8  :: beta, sumval
  integer :: ndim, i, j, n
  allocate(pivec(ndim))
  sumval = zero
  do i=1,ndim
    do n = 1, ndim
      sumval = sumval + t(n,i)/dsqrt(norm(n))
    enddo
    pivec(i) = (two**(beta/two)) * sumval
    sumval = zero
  enddo
  do i=1,ndim
    do j=i,ndim
      matl(i,j) = pivec(i)*pivec(j)
      matl(j,i) = pivec(j)*pivec(i)
    enddo
```

```
    enddo
    deallocate(pivec)
end subroutine

! diagonalization of complex symmetric matrix
subroutine call_zgeev_wt_eigvecs(h,ndim,eigvals,vecsl,vecsr)
    implicit none
    integer(kind = 4) :: ndim
    complex(kind = 8) :: h(ndim,ndim)
    complex(kind = 8) :: eigvals(ndim)
    complex(kind = 8) :: vecsl(ndim,ndim)
    complex(kind = 8) :: vecsr(ndim,ndim)
    integer(kind = 4) :: lda,ldvl,ldvr,ldwork
    integer(kind = 4) :: info
    complex(kind = 8),allocatable:: work(:),work2(:)
    character(len  = 1),parameter :: jobvl="v"
    character(len  = 1),parameter :: jobvr="v"
    lda = ndim
    ldvl= ndim
    ldvr= ndim
    ldwork=2*ndim
    allocate(work(ldwork),work2(ldwork))
    call zgeev(jobvl,jobvr,ndim,h,lda,eigvals,vecsl,ldvl,&
    vecsr,ldvr,work, ldwork, work2, info)
    deallocate(work,work2)
end

! diagonalization of real symmetric matrix
subroutine call_dsyev_wt_eigvecs(h,ndim,eigvals)
    implicit none
    integer   (kind = 4)  :: ndim
    real      (kind = 8)  :: h(ndim,ndim)
    real      (kind = 8)  :: eigvals(ndim)
    integer   (kind = 4)  :: lda
    integer   (kind = 4)  :: ldwork
    integer   (kind = 4)  :: info
    real      (kind = 8),allocatable:: work(:)
    character(len  = 1),parameter  :: jobz="v"
    character(len  = 1),parameter  :: uplo="l"
```

```
  lda = ndim
  ldwork=3*ndim-1
  allocate(work(ldwork))
  call dsyev(jobz,uplo,ndim,h,lda,eigvals,work,ldwork,info)
  deallocate(work)
end
```

Listing B.3: Subroutines to evaluate Siegert pseudostates